eNeuro

Research Article: New Research | Disorders of the Nervous System

Ablation of type-1 IFN signalling in hematopoietic cells confers protection following traumatic brain injury

Type-1 IFN signalling regulates TBI outcome.

Ila P. Karve[1], Moses Zhang[1], Mark Habgood[1], Tony Frugier[1], Kate M. Brody[1], Maithili Sashindranath[2], C Joakim Ek[1], Stephane Chappaz[3], Ben T. Kile[3], David Wright[4], Hong Wang[4], Leigh Johnston[4], Maria Daglas[2], Robert C. Ates[1], Robert L. Medcalf[2], Juliet M. Taylor[1] and Peter J. Crack[1]

[1]*Department of Pharmacology and Therapeutics, University of Melbourne, Parkville, Victoria, Australia, 3010*

[2]*Australian Centre for Blood Diseases, Monash University, Melbourne, Victoria, Australia, 3004*

[3]*ACRF Chemical Biology Division, The Walter and Eliza Hall Institute of Medical Research, Parkville, Victoria, Australia 3052*

[4]*Florey Imaging, The Florey Institute of Neuroscience and Mental Health, Parkville, Victoria, Australia 3052*

DOI: 10.1523/ENEURO.0128-15.2016

Received: 28 October 2015

Revised: 21 December 2015

Accepted: 14 January 2016

Published: 5 February 2016

Author contributions: I.K., M.Z., T.F., K.M.B., S.C., D.K.W., H.W., and P.J.C. performed research; I.K., T.F., M.S., J.E., S.C., D.K.W., M.D., J.M.T., and P.J.C. analyzed data; I.K., J.M.T., and P.J.C. wrote the paper; M.H., T.F., M.S., J.E., B.K., and P.J.C. contributed unpublished reagents/analytic tools; L.A.J., R.A., R.M., J.M.T., and P.J.C. designed research.

Funding: Department of Health, Australian Government | National Health and Medical Research Council (NHMRC): 501100000925; APP1044714. Australian Research Council;

Conflict of Interest: Authors report no conflict of interest.

National Health and Medical Research Council of Australia and the Australian Research Council.

Correspondence should be addressed to Corresponding author: Peter Crack, Department of Pharmacology and Therapeutics, University of Melbourne, Parkville, Victoria 3010, Australia. Phone: 613 8344 8417; Fax: 613 8344 0241; Email: pcrack@unimelb.edu.au

Cite as: eNeuro 2016; 10.1523/ENEURO.0128-15.2016

eNeuro

http://eneuro.msubmit.net

eN-NWR-0128-15R1

Ablation of type-1 IFN signalling in hematopoietic cells confers protection following traumatic brain injury.

1. Ablation of type-1 IFN signalling in hematopoietic cells confers protection following traumatic brain injury

2. Type-1 IFN signalling regulates TBI outcome.

3. Ila P Karve[1], Moses Zhang[1], Mark Habgood[1], Tony Frugier[1], Kate M. Brody[1], Maithili Sashindranath[2], C Joakim Ek[1], Stephane Chappaz[3], Ben T Kile[3], David Wright[4], Hong Wang[4], Leigh Johnston[4], Maria Daglas[2], Robert C Ates[1], Robert L Medcalf[2], Juliet M Taylor[1], Peter J Crack[1*].

[1] Department of Pharmacology and Therapeutics, University of Melbourne, Parkville, Victoria, Australia, 3010.

[2] Australian Centre for Blood Diseases, Monash University, Melbourne, Victoria, Australia, 3004.

[3] ACRF Chemical Biology Division, The Walter and Eliza Hall Institute of Medical Research, Parkville, Victoria, Australia 3052.

[4] Florey Imaging, The Florey Institute of Neuroscience and Mental Health, Parkville, Victoria, Australia 3052.

4. IPK – performed research, analysed data, wrote the paper
MZ – performed research
MH – contributed unpublished reagents/analytic tools
TF – contributed unpublished reagents/analytic tools
KMB – performed research
MS - contributed unpublished reagents/analytic tools
CJE – contributed unpublished reagents/analytic tools
SC – performed research
BTK - contributed unpublished reagents/analytic tools
DW – performed research, analysed data
HW – performed research
LJ – designed research
MD - contributed unpublished reagents/analytic tools
RCA – performed research
RLM – contributed unpublished reagents/analytic tools
JMT – designed research, analysed data, wrote paper
PJC – designed research, analysed data, wrote paper

5. Corresponding author
Associate Professor Peter Crack
Department of Pharmacology and Therapeutics,
University of Melbourne,
Parkville,
Victoria 3010,
Australia

Phone: 613 8344 8417
Fax: 613 8344 0241
Email: pcrack@unimelb.edu.au

6. Number of figures - 14
7. Number of tables - 2
8. Number of multimedia - 0
9. Number of words for abstract - 231
10. Number of words for Significance Statement - 116
11. Number of words for Introduction - 547
12. Number of words for Discussion - 1731

13. Acknowledgements – This work was supported by National Health and Medical Research Council of Australia Project Grant 628391 (PJC) and Project Grant 1044714 (PJC, JMT), an Australian Research Council Future Fellowship (PJC) and the Rebecca Cooper Foundation.

14. Conflict of Interest – Authors report no conflict of interest.

15. Funding sources - National Health and Medical Research Council of Australia and the Australian Research Council.

Abstract

Type-1 interferons (IFNs) are pleiotropic cytokines, that signal through the type-1 IFN receptor (IFNAR1). Recent literature has implicated the type-1 IFNs in disorders of the central nervous system. In this study, we have investigated the role of type-1 IFNs in neuro-inflammation following traumatic brain injury (TBI). Using a controlled cortical impact model, TBI was induced in 8-10 week-old male C57BL/6J WT and IFNAR1$^{-/-}$ mice and brains were excised to study infarct volume, inflammatory mediator release via qPCR analysis and immune cell profile via immunohistochemistry. IFNAR1$^{-/-}$ mice displayed smaller infarcts compared to WT mice after TBI. IFNAR1$^{-/-}$ mice exhibited an altered anti-inflammatory environment compared to WT mice, with significantly reduced levels of the pro-inflammatory mediators TNFα, IL-1β and IL-6, an up-regulation of the anti-inflammatory mediator IL-10 and an increased activation of resident and peripheral immune cells after TBI. WT mice injected intravenously with an anti-IFNAR1 blocking monoclonal antibody (MAR1) 1h before, 30 min after or 30min and 2d after TBI displayed significantly improved histological and behavioural outcome. Bone marrow chimeras demonstrated that the hematopoietic cells are a peripheral source of type-1 IFNs that drives neuro-inflammation and a worsened TBI outcome. Type-1 IFN mRNA levels were confirmed to be significantly altered in human post-mortem TBI brains. Taken together, these data demonstrate that type-1 IFN signalling is a critical pathway in the progression of neuro-inflammation and presents a viable therapeutic target for the treatment of TBI.

Significance Statement

This research article investigates the inflammatory effect of type-1 interferons (IFN) in traumatic brain injury (TBI), in both human and mice. IFNs have been traditionally associated with peripheral inflammatory responses. However, these molecules are also present in the central nervous system and we believe that they play a key role in the control of neuroinflammation. Our study shows that reducing type-1 IFN signalling, either by genetic ablation or by pharmacological intervention, has a beneficial effect on the outcome after TBI. IFN signalling is required for the brain to mount an inflammatory response to the insult of TBI. This study addresses key issues in type-1 IFN signalling and is a seminal discovery of their role in TBI.

Introduction

Traumatic brain injury (TBI) is the leading cause of death and disability in children and young adults in industrialised countries (Summers et al., 2009). There are currently no effective therapies clinically available to reduce the extent of tissue damage resulting from a TBI (McConeghy et al., 2012). TBIs are extremely heterogeneous with the extent of tissue damage highly dependent on the nature of the injury. However, a common feature of all TBIs is an initial primary lesion followed by a period of secondary tissue damage (Bramlett and Dietrich, 2004). The secondary damage seen in TBI results from complex morphological and biochemical changes in the brain that manifest following the initial impact and can last from days to weeks.

A prime player in the secondary expansion of tissue damage following TBI is neuro-inflammation (Greve and Zink, 2009). Neuro-inflammation is a complex phenomenon involving many different cell types and soluble factors and has been implicated as a common feature in many neuro-pathologies (Clausen et al., 2009; Pineau et al., 2010; Mikita et al., 2011; Wang et al., 2011). The involvement of astrocytes and resident microglia as well as peripherally invading cells adds to the complexity of TBI progression. A recent study investigating temporal neuro-pathological changes in humans following TBI found that neuro-inflammatory events continued for years after the initial injury and contributed to ongoing neuro-degeneration (Johnson et al., 2013). These ongoing neuro-pathological changes highlight the severity of the long-term consequences of neuro-inflammation following TBI. Therefore, a better understanding of the neuro-

128 inflammatory events elicited by TBI is needed to develop more effective
129 therapies towards limiting tissue damage and degeneration.
130
131 Type-1 interferons (IFNs) are pleiotropic cytokines that are involved in
132 responses to viral and microbial infections and cell proliferation (Pestka, 2007).
133 Type-1 IFNs bind to and activate the IFNα receptor (IFNAR), which is comprised
134 of type-1 interferon receptor 1 (IFNAR1) and IFNAR2 subunits (de Weerd et al.,
135 2007). Engagement of this receptor complex leads to signalling through the
136 canonical JAK-STAT pathway, resulting in the up-regulation of anti-viral and
137 anti-proliferative proteins, including pro-inflammatory cytokines and
138 chemokines and autocrine production of type-1 IFNs (IFNα and β) (Dai et al.,
139 2011). Recent evidence indicates that injury to the CNS leads to up-regulation of
140 type-1 IFN gene expression (Field et al., 2010). This finding suggests that type-1
141 IFNs may function as key mediators of the neuro-inflammatory response
142 following TBI.
143
144 In this study, we investigated the role of type-1 IFN signalling in a controlled
145 cortical impact (CCI) model of TBI. Using mice deficient in the IFNAR1 receptor
146 subunit (IFNAR1$^{-/-}$), we have demonstrated that blocking type-1 IFN signalling
147 confers neuro-protection after TBI, and significantly alters the neuro-
148 inflammatory milieu within the brain. Using a bone marrow chimeric approach,
149 we have demonstrated that type-1 IFN signalling is involved in a deleterious role
150 in hematopoietic cells to drive the neuro-inflammatory response following TBI.
151 Furthermore, intravenous administration of a monoclonal antibody targeting
152 IFNAR1 (MAR1) in mice is neuro-protective, with post-TBI administration

resulting in improved neurological function and decreased infarct size. Complementing this finding is data from human post-mortem brains following TBI that display increased type-1 IFN levels. In total, this data supports a detrimental role for type-1 IFN signalling following TBI, and also proposes that ablation of this signalling cascade promotes the development of an anti-inflammatory, neuro-protective environment within the brain.

160 **Methods**

161

162 **Animals**

163 All animal procedures were performed in accordance with the Author University
164 animal care committee's regulations. 8-10-week-old male mice (23±3 g) of a
165 C57BL/6J background were obtained from the Animal Resource Centre. IFNAR1^{-}
166 $^{/-}$ mice on a C57BL/6J background were previously generated at the Institute of
167 Reproduction and Development at Monash University and were a kind gift from
168 Professor Paul Hertzog (Hwang et al., 1995).

169

170 **Controlled cortical impact model**

171 Mice were anaesthetised with an intra-peritoneal injection of Ketamine
172 (100mg/kg, Parnell)/Xylazine (10mg/kg, Parnell). A sagittal scalp incision was
173 made to expose the underlying parietal skull. A 2 mm diameter plate of bone
174 (centred 1.5 mm posterior to bregma and 2.5 mm lateral to the midline) was
175 then removed using a Dremel 10.8V drill with a 0.8mm tip (Dremel, Europe) to
176 expose the underlying right parietal cortex. A 1.5mm deep impact into the
177 exposed cortex was made at 5m/s using the computer-controlled impactor
178 device (LinMot-Talk 1100). Following impact, the bone plate was replaced and
179 held in place with a small section of parafilm to cover the injury site. The skin
180 incision was then closed with sterile silk 5.0 metric sutures (Syneture Tyco
181 Healthcare). Mice were administered intra-peritoneal Buprenorphine (0.6
182 mg/kg, Reckitt Benckiser Healthcare) and placed on a heat mat for post-surgical
183 recovery. Sham operated controls underwent the same anesthesia, scalp incision
184 and bone plate removal, but were not injured.

185

186 **MAR1 antibody administration**

187 WT mice were intra-venously administered, in a blinded fashion, either a
188 monoclonal antibody targeted toward IFNAR1 (Anti-mouse interferon α/β
189 receptor [IFNAR1], Leinco Technologies Inc (MAR1), 0.5mg) or a monoclonal
190 antibody isotype control (IgG isotype control, Leinco Technologies Inc, 0.5mg)
191 either 1h prior to, or 30 min after TBI. In a separate cohort, WT mice were
192 administered MAR1 or IgG both 30 min and 2d after TBI.

193

194 **Behavioural analysis**

195 Neurological function post-TBI was assessed using DigiGait™ v 11.5 (Mouse
196 Specifics Inc.) apparatus, as previously described in (Sashindranath et al., 2012).
197 Mice were run on a transparent treadmill at a speed of 15cm/s both before
198 injury and 3h post-injury for 5s. Videos of paw placement were captured in the
199 ventral plane by the DigiGait™ software and analysed by the software. All
200 surgeries and behavioural analyses were performed in a blinded fashion. Gait
201 measurements were calculated as post: pre injury ratios of sham versus trauma
202 mice. All gait parameters for antibody-treated mice were presented as fold
203 change relative to untreated TBI values.

204

205 **Preparation of serial sections for staining and infarct analysis**

206 Mice were trans-cardially perfused after injury (or sham surgery) with 0.1%
207 heparinised Phosphate-Buffered Saline (Pfizer), followed by 4%
208 paraformaldehyde (PFA, Scharlab S.L.). For infarct analysis, brains were
209 collected 24h or 7d after TBI or sham surgery, paraffin-embedded, cut into 10μm

210 serial sections and mounted on glass slides (3 sections per slide). Every 10th slide
211 was stained with Haematoxylin and Eosin (H&E). Images of the infarct were
212 captured using an Olympus BX50 microscope fitted with a digital camera and
213 infarct areas were measured using Image J software (NIH). The volume of tissue
214 occupied by the infarct between successive pairs of serial sections across the
215 infarct site was calculated from the area measurements in each section and the
216 known distance between sections (300μm) and summed to determine total
217 infarct volume (Figure 1).
218
219 For immunohistochemistry, brains were dissected after perfusion at 6 and 24h
220 post injury or sham surgery and placed in 4% PFA for 2h and 10% sucrose
221 (Univar) in PBS overnight at 4 °C. Brains were then placed into Optimal Cutting
222 Temperature (OCT) medium (Tissue Tek) and frozen in Isopropanol on dry ice
223 for a brief period and stored at -80°C until required. Brains were cut into 20μm
224 fresh-frozen coronal serial sections using a Microm HM 525 cryostat.
225
226 **Immunohistochemistry**
227 Fresh frozen sections were incubated in 0.2% Triton X-100 (Sigma) in PBS for 20
228 min, and blocked for 30min in CAS block (Invitrogen). Primary antibodies were
229 diluted in 1% BSA (Bovogen) in PBS and slides incubated with the antibody
230 overnight at 4°C. The primary antibodies used were: CD206 (1:1000,
231 BioScientific), Fox3 (1:200, Abcam), GFAP (1:1000, Cell Signaling), pSTAT3
232 (Ser727, 1:50, Santa Cruz) and Iba-1 (1:200, Wako). Slides were washed in PBS
233 and incubated in an appropriate secondary antibody. Fluorescent secondary
234 antibodies (Alexa Fluor 594 anti-mouse and Alexa Fluor 488 anti-rabbit;

235 Invitrogen) were used at 1:1000 (diluted in PBS). Sections were mounted in
236 Vectashield with DAPI (Vector laboratories), and imaged under water immersion
237 on a Leica DMI 6000B fluorescence microscope. Tiled images were imaged on a
238 Zeiss Observer Z1 using Zen 2011 software. Quantification of GFAP and Iba-1
239 staining was performed using Image J software (NIH), as described in (Baruch et
240 al., 2014). The software generated fluorescence intensity values by tracing the
241 region of interest (infarct in the ipsilateral hemisphere). Arbitrary units were
242 defined in terms of strength of fluorescent signal. Tiled images were captured on
243 the same day for all groups that were to be compared. In addition, fluorescence
244 intensity analysis was done at the same time for groups that were to be
245 compared. The final intensity values were calculated by subtracting the area of
246 the selected region multiplied by the background fluorescence from the
247 fluorescence intensity of the region of interest: Fluorescence intensity (arbitrary
248 units) = Fluorescence intensity of R.O.I – (Area of selected region x Mean
249 fluorescence of background).
250
251 **Chimera development**
252 C57BL/6 CD45.1 or IFNAR1$^{-/-}$ mice were irradiated (11 Gy in 2 equal doses, 2–3
253 hours apart) to block hematopoietic cell production, as per (Downes et al., 2013)
254 with the heads of the mice shielded. Recipient animals were then intravenously
255 injected with 1 x 10^6 unfractionated bone marrow cells isolated from femurs of
256 un-manipulated C57BL/6 CD45.1 or IFNAR1$^{-/-}$ donor mice. Percentage
257 chimerism was determined 8 weeks after bone marrow transplantation using
258 flow cytometry to assess levels of blood leukocytes using CD45-specific
259 monoclonal antibodies. TBI surgeries were performed 3 weeks after assessing

260 levels of engraftment.

261

262 **Magnetic Resonance Imaging (MRI)**

263 MRI scans were performed for the chimera study using a Bruker 4.7 Tesla small
264 animal MRI scanner (Florey Institute of Neuroscience and Mental Health) to
265 quantify the progression of tissue damage, as described in (Crack et al., 2014).
266 Mice were anesthetized with approximately 3% isoflurane in a 1:1 mixture of
267 medical-grade air and oxygen. Anesthesia was maintained throughout scanning
268 with 0.25 to 1.5% isoflurane through a nosecone placed over the animal' s snout
269 and respiration was continuously monitored throughout the experiment with a
270 pressure-sensitive probe positioned under the animal' s diaphragm.
271 Anesthetized animals were laid supine on a purpose-built small-animal holder
272 and their heads fixed into position with ear and bite bars. A surface receiver coil
273 was placed over the animals' heads and the cradle was inserted into a
274 transmitter coil fixed inside a BGA12S-HP gradient set for imaging. The MRI
275 protocol consisted of a 3-plane localizer sequence followed by multi-echo T2 and
276 diffusion-weighted sequences. The total scanning time was kept to less than 2 h
277 per animal. Multi-echo T2 -weighted images were acquired using a rapid
278 acquisition, relaxation enhanced (RARE) sequence with RARE factor = 2;
279 repetition time = 2,500 ms; effective echo time (TEeff) = 10, 30, 50, 70, 90 and
280 110 ms; field of view (FOV) = 1.6 Å~ 1.6 cm^2 ; matrix = 192 Å~ 192; and 16 slices
281 with thickness = 0.5 mm. Volumetric analysis was carried out on T2-weighted
282 images using ITK SNAP software [(Yushkevich et al., 2006); www.itksnap.org].

283

284 **Analysis of human samples by qPCR**

285 All procedures were conducted in accordance with the Australian National
286 Health & Medical Research Council's (NHMRC) National Statement on Ethical
287 Conduct in Human Research (2007), the Victorian Human Tissue Act 1982, the
288 National
289 Code of Ethical Autopsy Practice, and the Victorian Government Policies and
290 Practices in Relation to Postmortem. Trauma brain samples from individuals
291 who had died following closed head injury and non-head trauma controls were
292 obtained from the Victorian Brain Bank Network (VBBN) (Frugier et al., 2009;
293 Frugier et al., 2011; Frugier et al., 2012). Detailed patient is outlined in Table 1.
294 The following Taqman® primers for the human tissue samples were obtained
295 from Applied Biosciences: IFNα (ID: Hs00256882_s1), IFNβ (ID:
296 Hs01077958_s1), IFNAR1 (ID: Hs01066118_m1), IFNAR2 (ID: Hs01022060_m1),
297 18S ribosomal RNA (ID: Hs99999901_s1) and UBC (Hs01871556_s1).
298
299 **Quantitative Real Time Polymerase Chain Reaction (qRT-PCR)**
300 Ipsilateral hemispheres were dissected 2, 4 and 24h after TBI or sham surgery,
301 and RNA was isolated using Trizol® (Invitrogen). 1 μg of cDNA was transcribed
302 from RNA using a high capacity cDNA reverse transcription kit (Applied
303 Biosystems). Taqman ® and SYBR ® Green primers were obtained from Applied
304 Biosciences and GeneWorks for mouse tissue samples. Ct values were obtained
305 for each sample, and relative transcript levels for each gene were calculated
306 using the $2^{-\Delta\Delta CT}$ method (Winer et al., 1999).
307
308 **Enzyme-linked Immunosorbent Assay (ELISA)**
309 Ipsilateral hemispheres were dissected after TBI or sham surgery. Tissue was

310 homogenised in Tris buffer (50mM Tris, 150mM NaCl, 1% Triton X-100,
311 Phospho-STOP and Protease inhibitor [Roche]; pH 7.4) and rotated at 4°C for 90
312 min. Samples were centrifuged at 2000 x g and supernatant was collected. To
313 determine protein concentration of samples, a Bradford assay was performed
314 according to manufacturer's instructions (BioRad). Murine IL-1β, IL-6 and IL-10
315 ELISAs were purchased from BD Biosciences. 100μg of protein was loaded per
316 well in duplicate. Protein concentrations of individual samples were determined
317 using a linear curve of muIL-1β, muIL-6 and muIL-10 standards (4-250pg/mL).
318
319 **Statistics**
320 Data are expressed as Mean ± SEM, and analysed using Graph Pad Prism 5.0
321 software. Kolmogorov-Smirnov test (with Lilliefors correction) was used to test
322 for normality within each group. For qPCR, ELISA and chimera infarct analysis, a
323 one-way or two-way Analysis of Variance (ANOVA) was performed where
324 appropriate followed by Dunnetts post-hoc analysis and Bonferroni's post-hoc
325 analysis, respectively. Infarct volume, fluorescence intensity values and Digigait™
326 behavioural data were analysed using an unpaired Student's t-test. A value of
327 $p<0.05$ was considered significant. Statistics summarised in table 2.

328 **Results**

329

330 *TBI induces type-1 IFN signalling in mice*

331 Firstly, we investigated the profile of IFN transcript regulation in ipsilateral
332 hemispheres after controlled cortical impact in mice lacking the type-1
333 interferon receptor, IFNAR1. IFNα expression was significantly higher in WT
334 mice 2h after TBI compared to IFNAR1$^{-/-}$ mice ($p<0.001$, Figure 2A). In addition,
335 an up-regulation of IFNβ was seen 24h after TBI in WT, when compared to
336 IFNAR1$^{-/-}$ mice ($p<0.05$, Figure 2A). This confirmed release of type-1 IFNs
337 following TBI in mice. Signal transducer and activator of transcription (STAT) 3
338 is a critical signal mediator in type-1 IFN signalling. STAT3 is phosphorylated or
339 activated in this signalling cascade (Taylor et al., 2014), and here, pSTAT3
340 expression was used to assess the extent of type-1 IFN downstream signalling
341 after TBI. pSTAT3 expression was assessed in neurons (stained with Fox3) and
342 glia (stained with GFAP) in the ipsilateral hemisphere of both WT and IFNAR1$^{-/-}$
343 mice (Figure 2B and C). Fox3 was chosen as a neuronal marker due to its
344 identification as the antigen for NeuN (neuronal nuclei) (Kim et al., 2009). 6h
345 after TBI, pSTAT3 expression was elevated in neuronal cells in the cortex of WT
346 mice compared to sham mice. In contrast, pSTAT3 expression could not be
347 detected in corresponding IFNAR1$^{-/-}$ sections. However, pSTAT3 expression was
348 detected in both the WT and IFNAR1$^{-/-}$ mice 24h after TBI and was co-localised
349 with Fox3. Similarly, immunostaining identified an increase in pSTAT3 in WT
350 mice 6h post TBI in glia, which was maintained 24h post TBI. IFNAR1$^{-/-}$ mice
351 demonstrated no pSTAT3 staining 6h post TBI, but showed pSTAT3
352 immunoreactivity 24h post TBI, some of which co-localised with glia. This

353 suggests STAT3 may be activated through alternate pathways at later time
354 points in the IFNAR1$^{-/-}$ after TBI. Additionally, we investigated interferon
355 regulatory factor 7 (IRF7) mRNA levels following TBI. IRF7 is a key protein
356 involved in type-1 IFN induction through various pathways, one of them being
357 the type-1 IFN pathway itself (Marie et al., 1998; Sato et al., 1998; Honda et al.,
358 2005). We identified an increase in IRF7 levels 2h post TBI in WT, but not
359 IFNAR1$^{-/-}$ mice ($p<0.01$, Figure 2A). This further confirmed activation of
360 downstream mediators of the type-1 IFN pathway in an IFNAR1-dependent
361 manner.
362
363 *Mice lacking the IFNAR1 subunit have smaller infarct volumes after TBI*
364 The role of IFNAR in neuro-protection after TBI was of particular interest given
365 we had established the involvement of type-1 IFN signalling in TBI in mice. To
366 investigate this, WT and IFNAR1$^{-/-}$ mice were given TBI, and infarct volumes
367 were measured in coronal H&E-stained brain sections taken 24h post-TBI. This
368 experimental focal model of TBI produced a lesion confined to the cortical region
369 of the ipsilateral hemisphere (Figure 3A). 24h after TBI, IFNAR1$^{-/-}$ mice had
370 significantly smaller infarct volumes compared to their WT counterparts
371 (3.52mm^3 compared to 6.96mm^3, respectively; $p=0.0047$, $n=6$; Figure 3B).
372
373 *IFNAR1$^{-/-}$ mice display lower pro-inflammatory, and higher anti-inflammatory*
374 *cytokine levels compared to WT mice after TBI*
375 To investigate the mechanism behind the neuro-protection seen in IFNAR1$^{-/-}$
376 mice, we investigated the expression profile of the pro-inflammatory genes IL-1β
377 and IL-6 and the anti-inflammatory cytokine IL-10 in the ipsilateral hemispheres

378 following TBI in both WT and IFNAR1$^{-/-}$ mice. mRNA levels of IL-1β were
379 significantly elevated in WT, compared to IFNAR1$^{-/-}$ mice at 2, 4 and 24h after
380 TBI ($p<0.05$ and $p<0.001$, n=3; Figure 4A). IL-6 was elevated in the ipsilateral
381 hemisphere WT mice 4h after TBI compared to controls, but this up-regulation
382 was not significantly different compared to the IFNAR1$^{-/-}$ mice at 4h (Figure 4B).
383 IFNAR1$^{-/-}$ mice demonstrated increased IL-10 mRNA levels compared to WT
384 mice both 2 and 4h after TBI ($p<0.05$, Figure 4C). To validate these data, we
385 performed ELISAs to detect protein levels of the same cytokines. IL-1β and IL-6
386 protein levels were elevated in WT, compared to IFNAR1$^{-/-}$ mice at 6h (IL-1β)
387 and 2h (IL-6; $p<0.05$, Figure 4D and 4E). IL-10 protein levels were elevated in
388 IFNAR1$^{-/-}$, compared to WT mice both 2 and 24h post TBI ($p<0.01$, Figure 4F).
389 These data imply signalling through IFNAR1 mediates the up-regulation of pro-
390 inflammatory genes post-TBI. In addition, absence of IFNAR1 results in an
391 increase in the anti-inflammatory cytokine, IL-10. This strongly suggests the
392 preference for a heightened anti-inflammatory and suppressed pro-
393 inflammatory response in these IFNAR1$^{-/-}$ mice.
394
395 *IFNAR1$^{-/-}$ mice display an increase in GFAP and Iba-1 staining compared to WT*
396 *mice*
397 Astrogliosis is a common feature of neuro-inflammatory pathologies, and is
398 characterised by an up-regulation in GFAP expression in astrocytes (Zamanian et
399 al., 2012). This response may be either protective or deleterious in various
400 pathologies (Terai et al., 2001; Paintlia et al., 2013). In WT and IFNAR1$^{-/-}$ mice
401 subjected to TBI, an increase in GFAP staining was seen compared to sham-
402 operated controls indicating a neuroinflammatory response elicited by the TBI

403 (data not shown). Interestingly, IFNAR1$^{-/-}$ mice displayed increased GFAP
404 staining (Figure 5A) and expression compared to WT mice 24h after TBI (492.2
405 compared to 313.9 arbitrary fluorescence intensity units, respectively, p=0.001,
406 n=5; Figure 5C). In addition, we performed immunohistochemistry to detect
407 activated microglia and peripherally invading macrophages. Ionised calcium
408 binding adapter molecule 1 (Iba-1) is expressed in both microglia and
409 macrophages (Fukuda et al., 1996), and its expression is up-regulated by the
410 activation of these cell types (microgliosis). Baseline Iba-1 levels were similar in
411 WT and IFNAR1$^{-/-}$ shams (data not shown), and were increased in both WT and
412 IFNAR1$^{-/-}$ mice following TBI compared to shams (Figure 6A). Additionally, we
413 observed a trend for increased Iba-1 immunoreactivity in IFNAR1$^{-/-}$ mice
414 compared to WT mice 24h after TBI (352.2 compared to 254.8 arbitrary
415 fluorescence intensity units, respectively, p=0.053, Figure 6C). In the IFNAR1$^{-/-}$
416 mice we were expecting to see decreased immunoreactivity of both GFAP and
417 Iba-1, however contrary to our hypothesis, we identified increased
418 immunoreactivity of both astrocytes (GFAP) and microglia/macrophages (Iba-1)
419 in IFNAR1$^{-/-}$ mice, suggestive of increased astro- and micro-gliosis. However, in
420 conjunction with this increased GFAP and Iba-1 cellular response, we identified a
421 decreased pro-inflammatory, and increased anti-inflammatory response (Figure
422 3). The M2 marker, CD206 was shown to have staining in the IFNAR1-/- brain
423 after TBI when compared to the WT that is suggestive of an altertered microglial
424 phenotype (Figure 7). Collectively, these data support the presence of a
425 dominant anti-inflammatory and potentially protective environment in the
426 IFNAR1$^{-/-}$ mice following TBI.
427

428 *MAR1, a monoclonal antibody targeted to IFNAR1, is effective at reducing infarct*
429 *volume when administered before and after TBI in mice*

430 The neuro-protective effects of knocking out IFNAR1 were confirmed by
431 administering an antibody to IFNAR1 (MAR1) to block the receptor either before
432 or after injury. Pre-treatment with MAR1 1h before injury resulted in
433 significantly smaller infarct volumes when compared to animals pre-treated with
434 an IgG isotype control (5.12mm^3 compared to 8.37mm^3, $p<0.0438$, n=3; Figure
435 8A). Post-treatment with MAR1 30 min after injury also resulted in smaller
436 infarct volumes compared to IgG isotype control-treated mice (5.77mm^3
437 compared to 9.23mm^3, $p=0.0001$, n=6; Figure 8B). Additionally, when mice were
438 treated with IgG or MAR1 both 30min and 2d after TBI, MAR1-treated mice had
439 smaller infarcts compared to IgG-treated mice 7d after TBI (8.50mm^3 compared
440 to 14.11mm^3, $p=0.035$, n=8; Figure 8C). These results indicate that blocking type-
441 1 IFN signalling is neuro-protective both over a short and long time course after
442 TBI, highlighting the therapeutic potential of MAR1 for TBI treatment.

443

444 *MAR1 administration results in decreased IFN levels and a dampened pro-*
445 *inflammatory response*

446 To investigate the mechanism of MAR1-elicited protection, we performed qPCR
447 and ELISAs to detect levels of IFN and the pro-inflammatory cytokines IL-1β and
448 IL-6. Again, we investigated changes in ipsilateral hemispheres of mice after TBI.
449 IFNα mRNA levels were increased in IgG-treated mice compared to MAR1-
450 treated mice 2h post TBI ($p<0.001$, Figure 9A). IFNβ mRNA levels were increased
451 in IgG-treated mice compared to MAR1-treated mice 4h after TBI ($p<0.05$, Figure
452 9B). Levels of IL-1β and IL-6 were higher in IgG-treated mice compared to

453 MAR1-treated mice 4h post TBI, as measured by ELISA ($p<0.05$, Figure 9C and
454 9D), interestingly IL-10 levels were found to be unchanged by MAR1 treatment
455 (Figure 9E). Similar to genetic ablation of IFNAR1, MAR1 administration
456 suppressed the signalling of type-1 IFNs and pro-inflammatory cytokines
457 following TBI.
458
459 *Post-TBI administration of MAR1 significantly improves neurological function in*
460 *injured mice*
461 To identify changes in neurological function in mice following TBI, the Digigait™
462 system and software were used. Injured mice displayed impaired locomotor
463 function in their left hind limb (contralateral limb to injury) compared to sham
464 operated control mice in parameters such as stance/swing ratio, % swing in
465 stride and % stance in stride 3h after TBI. Sham and TBI comparisons are
466 presented as post:pre injury ratios in Figures 10A-C. Changes in these gait
467 indices in the MAR1 antibody and IgG isotype-treated mice are presented as fold
468 change relative to untreated WT TBI mice. We found that administration of
469 MAR1 30 min post-TBI significantly improved locomotor function after TBI for
470 the left hindlimb in the parameters of stance/swing ratio (Figure 10D, $p=0.0124$,
471 $n=10$), % swing in stride (Figure 10E, $p=0.0156$, $n=10$) and % stance in stride
472 (Figure 10F, $p=0.0124$, $n=10$). These results indicate that MAR1 is an effective
473 treatment that improves neurological function and behavioural outcome after
474 TBI.
475
476 *Blocking type-1 IFN signalling in the hematopoietic cell compartment is protective*
477 *following traumatic brain injury*

478 In order to dissect the cellular mechanisms behind IFNAR1-mediated neuro-
479 inflammation, we generated bone marrow chimeras of WT C57BL/6 CD45.1 and
480 IFNAR1$^{-/-}$ mice. We performed TBI on 3 groups of mice: mice, which had IFNAR1
481 deleted, except in hematopoietic cells (WT→IFNAR1$^{-/-}$), mice, which had IFNAR1
482 deleted only in hematopoietic cells (IFNAR1$^{-/-}$→WT) and mice without IFNAR1
483 deletion (WT→WT). We assessed successful engraftment of donor cells using
484 flow cytometry. All groups of mice demonstrated >95% engraftment in CD19
485 positive blood B cells and approximately 80% engraftment of CD19 negative T
486 cells (data not shown). Engraftment levels were measured 8 weeks post
487 transplantation. The level of engraftment in T cells reflects the fact that the T
488 cells were largely resistant to the irradiation. WT radiation naïve mice displayed
489 similar infarct volumes to WT mice reconstituted with WT bone marrow (data
490 not shown). T2-weighted MRI demonstrated that the IFNAR1$^{-/-}$→WT group had
491 significantly lower infarct volumes 7d following injury, and displayed a trend for
492 a reduced infarct volume 24h following injury (Figure 11A, C). In comparison
493 there was no significant change in infarct volume in the WT→IFNAR1$^{-/-}$ group
494 (Figure 11B, C). This finding reveals a critical role for type-1 IFN signalling in
495 driving neuro-inflammation in peripheral hematopoietic cells following TBI.
496
497 *Type-1 interferon signalling in the hematopoietic compartment influences*
498 *astrogliosis and microgliosis.*
499 An increase in GFAP and Iba-1 staining was observed in TBI mice compared to
500 sham-operated chimeras (sham tiled images not shown). GFAP
501 immunoreactivity was unchanged between all chimera groups 24h after injury
502 when quantified as fluorescence intensity (data not shown). 7d post injury,

503 IFNAR1$^{-/-}$→WT mice displayed elevated GFAP levels compared to WT→WT and
504 WT→IFNAR1$^{-/-}$ mice (494.4 ± 36.5 arbitrary fluorescence units [IFNAR1$^{-/-}$→WT],
505 315.9 ± 34.6 arbitrary fluorescence units [WT→WT] and 404.9 ± 30.0 arbitrary
506 fluorescence units [WT→IFNAR1$^{-/-}$]; p=0.0273, Figure 12). Similarly, no
507 identifiable differences were observed with Iba-1 immunohistochemistry in
508 chimera groups at 24h (data not shown). Again, 7d post injury, IFNAR1$^{-/-}$→WT
509 mice displayed significantly elevated Iba-1 levels compared to the other two
510 groups (476.4 ± 24.2 arbitrary fluorescence units [IFNAR1$^{-/-}$→WT], 354.5 ± 8.7
511 arbitrary fluorescence units [WT→WT] and 389.3 ± 11.45 arbitrary fluorescence
512 units [WT→IFNAR1$^{-/-}$]; p<0.0047, Figure 13). Elevated GFAP and Iba-1 levels in
513 IFNAR1$^{-/-}$→WT chimeras could indicate an increased accumulation of reactive
514 astrocytes and microglia/macrophages in these mice, especially in the days
515 following injury.
516
517 *Type-1 interferons are involved in human TBI pathology*
518 To investigate the contribution of type-1 IFN signalling in humans following TBI,
519 we assessed type-1 IFN mRNA levels in post-mortem brains with qPCR (Figure
520 14). Details of human post-mortem tissue samples can be found in Table 1. A
521 decrease in IFNα mRNA levels was identified in subjects that had died 3h after
522 TBI (p=0.0019, Figure 14A). In contrast, IFNβ mRNA levels were significantly
523 increased in subjects that had died 6h after TBI compared to controls (p=0.0001,
524 Figure 14B). Levels of the receptor subunits IFNAR1 and IFNAR2 remained
525 unchanged in injured brains compared to controls, indicating the potential for
526 intact ligand-receptor interaction (Figure 14C). Type-1 IFNs are therefore

527 implicated in humans after TBI, demonstrating the relevance of studying this
528 system in neuro-inflammation following TBI.
529

530 **Discussion**

531 The current data show that ablation of IFN signalling through genetic deletion of
532 IFNAR1 or pharmacological blockade of the receptor leads to pronounced
533 protection after TBI. Previous studies have documented the roles of type-1 IFNs
534 in responses to viral and tumour-associated pathologies (Hwang et al., 1995;
535 Henry et al., 2007) but this is the first study to implicate type-1 IFN signalling in
536 *in vivo* acute neural injury. Type-1 IFNs are known to be released in response to
537 cellular stress via toll-like receptor (TLR) pathways (Field et al., 2010),
538 contributing to further damage and neuro-degeneration (Taylor et al., 2014). The
539 role of type-1 IFNs in the CNS is an emerging field of study, with recent evidence
540 suggesting that the type-1 IFN response contributes to the pathology seen in
541 acute and chronic neuro-pathologies (Khorooshi and Owens, 2010; Wang et al.,
542 2011; Taylor et al., 2014).
543
544 Our study highlights the involvement of type-1 IFN signalling in both mice and
545 humans following TBI. We reported IFNAR1-dependent increases in IFNα and
546 IFNβ after TBI in mice. In addition to primary type-1 IFN induction, it is known
547 that type-1 IFNs are also produced through IFNAR signalling as a positive
548 feedback mechanism (Gough et al., 2010). It is also possible that IFNAR drives
549 the secondary production of these IFNs leading to the exacerbation of
550 inflammation in humans. Interestingly, IFNα was elevated early in mice,
551 contrasting to the down-regulation in IFNα mRNA in human TBI patients. In
552 addition to this, IFNβ was elevated in humans to a greater extent than that seen
553 in mice. The disparity between the human and murine results may be explained
554 as the initiator of the neuro-inflammatory cascade may differ; being IFNβ in

555 humans and IFNα in mice. The production of IFNs is under tight regulation by
556 IFN-producing pathways. It has been established that murine type-1 IFN release
557 is controlled largely by the transcription factor IRF7 (Honda et al., 2005). A
558 recent study in human blood monocytes demonstrated that IFNβ production was
559 under joint control of the transcription factors IRF3 and IRF8 (Li et al., 2011).
560 While these studies were conducted in models of infection, they do suggest that
561 the regulation of type-1 IFN induction differs between mice and humans; hence
562 the production of these cytokines will be influenced largely by which IRFs are
563 dominant following infection or injury.
564
565 Downstream activation of type-1 IFN signalling was further confirmed after TBI
566 with pSTAT3 immunohistochemistry and IRF7 induction. STAT3, a transcription
567 factor, has broad roles in cell cycle regulation, and can be activated via IFN
568 signalling pathways (Taylor et al., 2014). Recently, STAT3 phosphorylation was
569 identified in astrocytes in a rat fluid percussion injury model of TBI where it was
570 proposed that activation of STAT3 could contribute to inflammation or be
571 neuroprotective depending on cell type (Oliva et al., 2011). In addition, STAT3
572 was found to be phosphorylated in an IFNAR1-dependent manner in a model of
573 Alzheimer's disease, identifying STAT3 as a crucial downstream effector of type-
574 1 IFN signalling (Taylor et al., 2014). In our CCI model, it was found that STAT3
575 was phosphorylated in GFAP-positive astrocytes and Fox3-positive neurons 6h
576 following injury in an IFNAR1-dependent manner. This activation was absent in
577 IFNAR1-/- brains. Our findings support a role for STAT3 as a critical
578 downstream mediator of type-1 IFN signalling following CNS injury. In addition,
579 IRF7 was induced 2h following TBI in WT, but not IFNAR1$^{-/-}$ mice. IRF7 is

implicated in type-1 IFN production and signalling, and it has been shown that absence of IRF7 impairs IFNα and β production (Honda et al., 2005). In a study of hippocampal sterile injury, type-1 IFN signalling pathways were activated via IRF7, leading to the release of downstream inflammatory mediators (Khorooshi and Owens, 2010). Collectively, our results point to an engagement and activation of type-1 IFN signalling pathways following TBI.

Downstream of type-1 IFN pathway activation, we investigated the release of pro-inflammatory mediators IL-1β [illegible] IL-6. Type-1 IFN signalling influenced the release of these mediators, with diminished levels of IL-1β mRNA and both IL-1β and IL-6 protein in the IFNAR1$^{-/-}$ mice. The neutralisation of pro-inflammatory cytokines has often been associated with beneficial outcomes post-TBI (Clausen et al., 2009). Additionally, studies investigating therapeutics targeting inflammation post-TBI often report decreases in pro-inflammatory cytokine levels (Truettner et al., 2005; Lloyd et al., 2008). Taken together, this evidence proposes that suppression of the pro-inflammatory response in the IFNAR1$^{-/-}$ mice after TBI could explain a potential mechanism as to why these mice exhibit decreased lesion volumes.

Another crucial hallmark of the neuro-inflammatory cascade in TBI is the activation of resident astrocytes and microglia, and infiltration of peripheral immune cells (D'Mello et al., 2009; Pineau et al., 2010; Zamanian et al., 2012; Wang et al., 2013). Astrocytes are crucial in regulating responses to infection and neural injury, and respond to such challenges by becoming 'reactive' and up-regulating expression of glial fibrillary acidic protein (GFAP), in a process termed

605 astrogliosis (Zamanian et al., 2012). Astrogliosis has been defined in the context
606 of both neuro-degeneration and neuro-protection in the CNS, and reactive
607 astrocytes are known to produce mediators such as pro- and anti-inflammatory
608 cytokines and growth factors to elicit their effects onto the surrounding
609 environment (Myer et al., 2006; Zamanian et al., 2012). Similarly, microglial cells
610 can also undergo reactive gliosis under conditions of cellular stress or injury
611 (Cao et al., 2012). In contrast to our results reporting decreased pro-
612 inflammatory cytokines, we observed increased GFAP and Iba-1 staining in the
613 IFNAR1$^{-/-}$ mouse after TBI, indicative of increased astro- and microgliosis.
614 Interestingly however, this increased gliosis in IFNAR1$^{-/-}$ mice was observed
615 concomitantly with diminished levels of pro-inflammatory mediators, and
616 elevated levels of anti-inflammatory IL-10, suggestive of an 'M2-like' or
617 reparative glial response to injury.
618
619 The Iba-1 antibody is known to detect both microglia and peripherally invading
620 macrophages, therefore it is reasonable to expect the detection of both cell types
621 in our TBI model. A recent study conducted in a mouse compression injury
622 model of TBI demonstrated that an acute inflammatory response coordinated
623 primarily by microglia, macrophages and neutrophils is neuro-protective and
624 limits cell death within the meninges and deeper brain tissue (Roth et al., 2014).
625 The increase in microglia and macrophages found in the IFNAR1$^{-/-}$ mice
626 following TBI may be eliciting a similar neuro-protective function. Similar to the
627 astrocytes in the IFNAR1$^{-/-}$ mice, activated microglia/macrophages in the
628 absence of IFNAR1 may lack the ability to produce pro-inflammatory cytokines.
629 This may explain why IFNAR1$^{-/-}$ mice have a dramatically reduced cytokine load

630 after TBI. These results highlight the possibility of distinctive differences in the
631 neuro-inflammatory milieu between WT and IFNAR1$^{-/-}$ mice after TBI.
632
633 Our results suggest that the IFNAR1$^{-/-}$ mice demonstrate a greater M2-polarised
634 environment compared to WT mice after TBI. This is highlighted by an up-
635 regulation of IL-10 mRNA and protein levels in IFNAR1$^{-/-}$ mice compared to WT
636 mice after TBI. IL-10 is an anti-inflammatory cytokine, and is produced by
637 immune cells undergoing a phenotypic switch from 'resting' to 'alternatively
638 activated.' Consequently, IL-10 is used as an M2 marker (Wang et al., 2013).
639 These alternately activated cells exhibit anti-inflammatory, pro-angiogenic
640 features, and up-regulate various different cytokines and growth factors (Sica et
641 al., 2006). In a mid cerebral artery (MCAO) model of stroke, IL-10 administration
642 was found to suppress overexpression of pro-inflammatory mediators IFNγ and
643 TNFα and reduce lesion volume (Liesz et al., 2009). Furthermore, IL-10
644 administration in a mouse model of TBI improved neurological recovery post-
645 TBI, and was associated with reduced levels of TNFα and IL-1β expression in the
646 cortex and hippocampus (Knoblach and Faden, 1998). These studies
647 demonstrate that an increased anti-inflammatory environment via increased IL-
648 10 can result in a shift towards suppression of a pro-inflammatory environment
649 and consequent protection and may explain how increased IL-10 levels in the
650 IFNAR1$^{-/-}$ after TBI contributes to the resultant neuroprotection.
651
652 Additional to silencing type-1 IFN signalling genetically, we demonstrated
653 protective effects of administering a blocking monoclonal antibody, MAR1.
654 MAR1-treated WT mice demonstrated reduced infarct volumes, similar to

655 IFNAR1$^{-/-}$ mice. Furthermore, administration of MAR1 resulted in decreased
656 production of the pro-inflammatory cytokines IL-1β and IL-6. Secondary
657 production of the type-1 IFNs, IFNα and β, was also blocked by MAR1
658 administration. Finally, MAR1 treatment improved behavioural outcome in WT
659 mice after TBI. Collectively, these results suggest that MAR1 treatment is
660 effective at managing TBI-induced neuro-inflammation, leading to a beneficial
661 post-traumatic outcome, and indicates its potential as a viable therapeutic for
662 combating TBI. There is little doubt that in our model of TBI which has a
663 disrupted blood brain barrier that the MAR-1 antibody is able to cross readily in
664 to the brain. Whether this will occur with an intact barrier is unknown at this
665 time. It is known that some monoclonal antibodies are able to enter the brain
666 (Yu et al., 2011). What we do know from our bone marrow chimera experiments
667 is that the hematopoietic compartment influences TBI outcome and IFNAR1
668 signalling is heavily implicated. This data suggests that it is possible that MAR1
669 does not need to cross the barrier, and it's peripheral effects on type-1 IFN
670 signaling contribute to neuroprotection in TBI. Future studies are underway to
671 address this interesting mechanistic question.
672
673 To further investigate the cellular mechanisms leading to protection following
674 TBI in the IFNAR1$^{-/-}$ mice, bone marrow chimeras were generated. Through the
675 development of bone marrow chimeras, we ascertained that removal of type-1
676 IFN signalling in hematopoietic cells conferred protection after TBI. This finding
677 proposes that hematopoietic cells are a large contributor to the deleterious
678 aspects of type-1 IFN signalling after TBI. Many studies have utilised chimeric
679 approaches to investigate the relative contribution of brain-derived and

680 peripheral cells in injury responses (Chen et al., 2012; Downes et al., 2013).
681 These studies have implicated various inflammatory pathways, in both resident
682 and peripheral immune cells after injury. The distinction between these two
683 tissue compartments is an important factor to consider when trialling
684 therapeutics for acute brain injuries. Furthermore, targeting novel
685 neuroprotectants to cell types outside of the CNS may extend the window of
686 therapeutic opportunity in the treatment of TBI.
687
688 We have clearly demonstrated a critical role for type-1 IFN signalling in TBI.
689 Importantly, removal of type-1 IFN signalling, both genetically and
690 pharmacologically confers protection after TBI. Detailed investigation into this
691 response after TBI indicates that signalling in peripheral immune cells is crucial
692 in driving the deleterious neuro-inflammatory cascade. Therefore, it is evident
693 that specific targeting of the peripheral component of the type-1 IFN response
694 represents a promising therapeutic option after brain injury.
695
696

697 **Figure 1: Photomicrographs showing the full extent of the infarct in an 8-10**
698 **week-old C57BL6/J WT mouse.** Images are of 10μm thick H&E-stained
699 sections from a mouse perfused 24h after injury. Sections are labeled s10-s100.
700 Damaged tissue is defined by a decrease in H&E staining intensity and an
701 example of border demarcation is illustrated in these images. Scale bar
702 represents 20μm.
703
704 **Figure 2- TBI induces type-1 IFN release and downstream STAT3/IRF7**
705 **activation in an IFNAR1-dependent manner. A** IFNα and IFNβ mRNA levels
706 are elevated in ipsilateral hemispheres of WT, compared to IFNAR1$^{-/-}$ mice 2 and
707 24h following TBI, respectively. Data represent mean± SEM, n=3 per group,
708 *p<0.05, ***p<0.001. **B** pSTAT3 immunoreactivity is observed 6h following TBI
709 in WT, but not IFNAR1$^{-/-}$ neuronal cells (labelled with Fox3) in the ipsilateral
710 hemispheres compared to sham-operated mice. pSTAT3 induction is
711 demonstrated in both WT and IFNAR1$^{-/-}$ neurons 24h after TBI. **C** 6h after TBI,
712 pSTAT3 expression is increased in WT, but not IFNAR1$^{-/-}$ mouse astrocytes
713 (labelled with GFAP) in the ipsilateral hemispheres compared to sham-operated
714 controls. pSTAT3 is expressed in both WT and IFNAR1$^{-/-}$ astrocytes 24h after
715 TBI. Images are representative of n=3 independent experiments. Scale bar
716 represents 50μm. **D** IRF7 mRNA levels are elevated in ipsilateral hemispheres of
717 WT, compared to IFNAR1$^{-/-}$ mice 2h following TBI. Data represent mean± SEM,
718 n=3 per group, **p<0.01.
719
720 **Figure 3- Absence of IFNAR1 contributes to a smaller infarct volume in**
721 **mice 24 hours after TBI. A** Representative 10μm thick Haematoxylin and Eosin

722 (H&E) stained coronal brain section from a WT and IFNAR1$^{-/-}$ mouse given TBI.
723 **B** IFNAR1$^{-/-}$ mice have significantly reduced infarct volumes compared to WT
724 mice 24h after TBI. Data represent mean ± SEM, *p<0.05, n=6 animals per group.
725 Scale bar represents 2mm.
726
727 **Figure 4- IFNAR1$^{-/-}$ mice display lower levels of pro-inflammatory**
728 **cytokines and higher levels of the anti-inflammatory cytokine IL-10 in**
729 **ipsilateral hemispheres compared to WT mice after TBI.** **A** IL-1β mRNA
730 levels are elevated at 2, 4 and 24h after TBI in WT, but not IFNAR1$^{-/-}$ mice. **B** IL-6
731 mRNA levels are elevated 4h after TBI in both WT and IFNAR1$^{-/-}$ mice. **C** IL-10
732 mRNA levels are elevated 2 and 4h after TBI in IFNAR1$^{-/-}$ compared to WT mice.
733 **D** WT mice display elevated IL-1β protein compared to IFNAR1$^{-/-}$ mice 6h after
734 TBI. **E** IL-6 protein levels are elevated in WT, compared to IFNAR1$^{-/-}$ mice 2h
735 after TBI. **F** IFNAR1$^{-/-}$ mice display higher levels of IL-10 protein compared to
736 WT mice 2 and 24h after TBI. Data represent mean ± SEM, n=3 per group,
737 *p<0.05, **p<0.01, ***p<0.001.
738
739 **Figure 5- IFNAR1$^{-/-}$ mice exhibit increased GFAP staining compared to WT**
740 **mice after TBI.** **A** Representative image of GFAP staining in the ipsilateral
741 hemisphere of WT and IFNAR1$^{-/-}$ mice 24h after TBI. Scale bar represents
742 200μm. **B** High resolution image of GFAP staining in the ipsilateral hemisphere of
743 WT and IFNAR1$^{-/-}$ mice 24h after TBI. Image region is outlined in the white box
744 in panel A. Scale bar represents 50μm. **C** Quantification of GFAP staining in TBI
745 mice, using fluorescence intensity values to quantify GFAP levels. Data represent
746 mean ± SEM, n=5 per group, **p<0.01.

747

748 **Figure 6 - Iba-1 levels increase after TBI, and are influenced by type-1 IFN**
749 **signalling. A** Representative image of Iba-1 staining in the ipsilateral
750 hemisphere of WT and IFNAR1$^{-/-}$ mice 24h after TBI. Scale bar represents
751 200µm. **B** High resolution image of Iba-1 staining in the ipsilateral hemisphere of
752 WT and IFNAR1$^{-/-}$ mice 24h after TBI. Image region is outlined in the white box
753 in panel A. Scale bar represents 50µm. **C** Quantification of Iba-1 staining in TBI
754 mice, using fluorescence intensity values to quantify Iba-1 levels. Data represent
755 mean ± SEM, n=5 per group, p=0.0537.
756

757 **Figure 7 – IFNAR1$^{-/-}$ microgila exhibit increased CD206 staining compared**
758 **to WT mice after TBI.** CD206 immunoreactivity is observed following TBI in
759 IFNAR1-/- mice at a greater level compared to WT mice 24 hrs after TBI. CD206
760 immunoreactivity is co-labelled with the microglial marker Iba-1.
761

762 **Figure 8- Pre- and post-treatment with MAR1 decreases infarct volume in**
763 **WT mice given TBI both 24h and 7d after TBI.**
764 **A** WT mice were treated 1h before surgery with MAR1 (0.5mg) or an IgG isotype
765 control (0.5mg); infarct was calculated 24h after TBI. Data represent mean ±
766 SEM, *p<0.05, n=3 animals per group. **B** WT mice were treated 30 min after TBI
767 with MAR1 or an IgG isotype control; infarct was calculated 24h after TBI. Data
768 represent mean ± SEM, *p<0.05, n=6 animals per group. **C** WT mice were treated
769 30 min and 2d after TBI with MAR1 or an IgG isotype control; infarct was
770 calculated 7d after TBI. Data represent mean ± SEM, *p<0.05, n=8 animals per
771 group.
772

773 **Figure 9- MAR1-treated mice display reduced type-1 IFN and pro-**
774 **inflammatory cytokine secretion following TBI. A** IFNα mRNA levels are
775 elevated in IgG-treated mice, compared to MAR1-treated mice 2h after TBI. **B**
776 IFNβ mRNA levels are elevated in IgG-treated mice, compared to MAR1-treated
777 mice 4h after TBI. **C** IL-1β protein levels are elevated in IgG-treated mice,
778 compared to MAR1-treated mice 4h after TBI. **D** IL-6 protein levels are elevated
779 in IgG-treated mice, compared to MAR1-treated mice 4h after TBI. **E** IL-10
780 protein levels are unchanged by MAR1 treatment after TBI. Data represent mean
781 ± SEM, n=3 per group, *p<0.05, ***p<0.001.
782
783 **Figure 10- MAR1 post-treatment significantly improves behavioural**
784 **outcome after TBI.** 3h after surgery, TBI mice show significant behavioural
785 impairment compared to sham mice in left hindlimb parameters such as
786 stance/swing ratio, % swing in stride and % stance in stride (**A-C**). Data are
787 presented as values of post:pre injury ratios. Post-TBI administration of MAR1
788 significantly improves behavioural outcome compared to IgG-treated mice in
789 these parameters (**D-F**). MAR1 and IgG-treated values are presented as fold
790 change to TBI. Data represent mean± SEM, *p<0.05, n=10 animals per group.
791
792 **Figure 11- Blocking type-1 IFN signalling in hematopoietic cells engenders**
793 **protection following TBI. A** MRI T2 images from bone marrow chimeric mice
794 showing TBI lesion 24h after injury. WT→WT mice represent C57BL/6 CD45.1
795 mice irradiated to abolish hematopoietic cells and reconstituted with BL/6 bone
796 marrow. IFNAR1$^{-/-}$→WT mice represent irradiated C57BL/6 CD45.1 mice
797 reconstituted with IFNAR1$^{-/-}$ bone marrow. WT→IFNAR1$^{-/-}$ mice represent

798 irradiated IFNAR1$^{-/-}$ mice reconstituted with C57BL/6 CD45.1 bone marrow.
799 Scale bar represents 1mm. **B** MRI T2 images from chimeric mice showing TBI
800 lesion 7 days after injury.
801 **C** IFNAR1$^{-/-}$→WT mice have significantly reduced infarct volumes 7 days after
802 injury. Data represent mean± SEM, **p<0.01, n=6-8 animals per group.
803
804 **Figure 12- GFAP immunoreactivity is significantly elevated in IFNAR1$^{-/-}$**
805 **→WT mice 7d after TBI. A** Representative tiled images using GFAP
806 immunohistochemistry in chimera groups 7d after TBI. Scale bar represents
807 200µm. **B** High resolution image of GFAP staining in the ipsilateral hemisphere of
808 all chimeras 7d after TBI. Image region is outlined in the white box in panel A.
809 Scale bar represents 50µm. **C** Quantification of GFAP staining in TBI mice, using
810 fluorescence intensity values to quantify GFAP levels. Data represent mean ±
811 SEM, n=3 per group, *p=0.0273.
812
813 **Figure 13- Iba-1 immunoreactivity is significantly elevated in IFNAR1$^{-/-}$**
814 **→WT mice 7d after TBI. A** Representative tiled images using Iba-1
815 immunohistochemistry in chimera groups 7d after TBI. Scale bar represents
816 200µm. **B** High resolution image of Iba-1 staining in the ipsilateral hemisphere of
817 all chimeras 7d after TBI. Image region is outlined in the white box in panel A.
818 Scale bar represents 50µm. **C** Quantification of Iba-1 staining in TBI mice, using
819 fluorescence intensity values to quantify Iba-1 levels. Data represent mean ±
820 SEM, n=3 per group, **p=0.0047.
821

822 **Figure 14- Type-1 IFN transcript levels are altered in humans after TBI,**
823 **while receptor levels are unchanged. A** IFNα mRNA levels are decreased
824 compared to control in patients who died <3h after TBI. **B** IFNβ mRNA levels are
825 elevated compared to control in patients who died >6h after TBI. **C** IFNAR1 and
826 IFNAR2 mRNA levels are unchanged in post-mortem brains. Samples were taken
827 from the ipsilateral hemisphere of these patients. Samples from the contralateral
828 hemisphere of patients who died >6h after TBI are represented in the last bar
829 (>6h CL). Data represent mean ± SEM, n=5-11 patients per group, *p<0.05.
830
831

832 **References**

833 Bramlett HM, Dietrich WD (2004) Pathophysiology of cerebral ischemia and
834 brain trauma: similarities and differences. J Cereb Blood Flow Metab
835 24:133-150.
836 Cao T, Thomas TC, Ziebell JM, Pauly JR, Lifshitz J (2012) Morphological and
837 genetic activation of microglia after diffuse traumatic brain injury in the
838 rat. Neuroscience 225:65-75.
839 Chen Z, Jalabi W, Shpargel KB, Farabaugh KT, Dutta R, Yin X, Kidd GJ, Bergmann
840 CC, Stohlman SA, Trapp BD (2012) Lipopolysaccharide-induced microglial
841 activation and neuroprotection against experimental brain injury is
842 independent of hematogenous TLR4. J Neurosci 32:11706-11715.
843 Clausen F, Hanell A, Bjork M, Hillered L, Mir AK, Gram H, Marklund N (2009)
844 Neutralization of interleukin-1beta modifies the inflammatory response
845 and improves histological and cognitive outcome following traumatic
846 brain injury in mice. Eur J Neurosci 30:385-396.
847 Crack PJ, Zhang M, Morganti-Kossmann MC, Morris AJ, Wojciak JM, Fleming JK,
848 Karve I, Wright D, Sashindranath M, Goldshmit Y, Conquest A, Daglas M,
849 Johnston LA, Medcalf RL, Sabbadini RA, Pebay A (2014) Anti-
850 lysophosphatidic acid antibodies improve traumatic brain injury
851 outcomes. J Neuroinflammation 11:37.
852 D'Mello C, Le T, Swain MG (2009) Cerebral microglia recruit monocytes into the
853 brain in response to tumor necrosis factoralpha signaling during
854 peripheral organ inflammation. J Neurosci 29:2089-2102.
855 Dai P, Cao H, Merghoub T, Avogadri F, Wang W, Parikh T, Fang CM, Pitha PM,
856 Fitzgerald KA, Rahman MM, McFadden G, Hu X, Houghton AN, Shuman S,
857 Deng L (2011) Myxoma virus induces type I interferon production in
858 murine plasmacytoid dendritic cells via a TLR9/MyD88-, IRF5/IRF7-, and
859 IFNAR-dependent pathway. J Virol 85:10814-10825.
860 de Weerd NA, Samarajiwa SA, Hertzog PJ (2007) Type I interferon receptors:
861 biochemistry and biological functions. The Journal of biological chemistry
862 282:20053-20057.
863 Downes CE, Wong CH, Henley KJ, Guio-Aguilar PL, Zhang M, Ates R, Mansell A,
864 Kile BT, Crack PJ (2013) MyD88 is a critical regulator of hematopoietic
865 cell-mediated neuroprotection seen after stroke. PLoS One 8:e57948.
866 Field R, Campion S, Warren C, Murray C, Cunningham C (2010) Systemic
867 challenge with the TLR3 agonist poly I:C induces amplified IFNalpha/beta
868 and IL-1beta responses in the diseased brain and exacerbates chronic
869 neurodegeneration. Brain, behavior, and immunity 24:996-1007.
870 Frugier T, Morganti-Kossmann C, O'Reilly D, McLean C (2009) In situ detection of
871 inflammatory mediators in post-mortem human brain tissue
872 following traumatic injury. J Neurotrauma.
873 Frugier T, Conquest A, McLean C, Currie P, Moses D, Goldshmit Y (2012)
874 Expression and Activation of EphA4 in the Human Brain After Traumatic
875 Injury. Journal of neuropathology and experimental neurology.
876 Frugier T, Crombie D, Conquest A, Tjhong F, Taylor C, Kulkarni T, McLean C,
877 Pebay A (2011) Modulation of LPA receptor expression in the human
878 brain following neurotrauma. Cell Mol Neurobiol 31:569-577.

879 Fukuda S, Tomatsu S, Masuno M, Ogawa T, Yamagishi A, Rezvi GM, Sukegawa K,
880 Shimozawa N, Suzuki Y, Kondo N, Imaizumi K, Kuroki Y, Okabe T, Orii T
881 (1996) Mucopolysaccharidosis IVA: submicroscopic deletion of 16q24.3
882 and a novel R386C mutation of N-acetylgalactosamine-6-sulfate sulfatase
883 gene in a classical Morquio disease. Hum Mutat 7:123-134.
884 Gough DJ, Messina NL, Hii L, Gould JA, Sabapathy K, Robertson APS, Trapani JA,
885 Levy DE, Hertzog PJ, Clarke CJP, Johnstone RW (2010) Functional
886 Crosstalk between Type I and II Interferon through the Regulated
887 Expression of STAT1. Plos Biol 8.
888 Greve MW, Zink BJ (2009) Pathophysiology of traumatic brain injury. Mt Sinai J
889 Med 76:97-104.
890 Henry T, Brotcke A, Weiss DS, Thompson LJ, Monack DM (2007) Type I
891 interferon signaling is required for activation of the inflammasome during
892 Francisella infection. J Exp Med 204:987-994.
893 Honda K, Yanai H, Takaoka A, Taniguchi T (2005) Regulation of the type I IFN
894 induction: a current view. International immunology 17:1367-1378.
895 Hwang SY, Hertzog PJ, Holland KA, Sumarsono SH, Tymms MJ, Hamilton JA,
896 Whitty G, Bertoncello I, Kola I (1995) A null mutation in the gene
897 encoding a type I interferon receptor component eliminates
898 antiproliferative and antiviral responses to interferons alpha and beta
899 and alters macrophage responses. Proceedings of the National Academy
900 of Sciences of the United States of America 92:11284-11288.
901 Johnson VE, Stewart JE, Begbie FD, Trojanowski JQ, Smith DH, Stewart W (2013)
902 Inflammation and white matter degeneration persist for years after a
903 single traumatic brain injury. Brain : a journal of neurology 136:28-42.
904 Khorooshi R, Owens T (2010) Injury-induced type I IFN signaling regulates
905 inflammatory responses in the central nervous system. J Immunol
906 185:1258-1264.
907 Kim KK, Adelstein RS, Kawamoto S (2009) Identification of neuronal nuclei
908 (NeuN) as Fox-3, a new member of the Fox-1 gene family of splicing
909 factors. The Journal of biological chemistry 284:31052-31061.
910 Knoblach SM, Faden AI (1998) Interleukin-10 improves outcome and alters
911 proinflammatory cytokine expression after experimental traumatic brain
912 injury. Experimental neurology 153:143-151.
913 Li P, Wong JJ, Sum C, Sin WX, Ng KQ, Koh MB, Chin KC (2011) IRF8 and IRF3
914 cooperatively regulate rapid interferon-beta induction in human blood
915 monocytes. Blood 117:2847-2854.
916 Liesz A, Suri-Payer E, Veltkamp C, Doerr H, Sommer C, Rivest S, Giese T,
917 Veltkamp R (2009) Regulatory T cells are key cerebroprotective
918 immunomodulators in acute experimental stroke. Nature medicine
919 15:192-199.
920 Lloyd E, Somera-Molina K, Van Eldik LJ, Watterson DM, Wainwright MS (2008)
921 Suppression of acute proinflammatory cytokine and chemokine
922 upregulation by post-injury administration of a novel small molecule
923 improves long-term neurologic outcome in a mouse model of traumatic
924 brain injury. J Neuroinflammation 5:28.
925 Marie I, Durbin JE, Levy DE (1998) Differential viral induction of distinct
926 interferon-alpha genes by positive feedback through interferon
927 regulatory factor-7. EMBO J 17:6660-6669.

928 McConeghy KW, Hatton J, Hughes L, Cook AM (2012) A review of
929 neuroprotection pharmacology and therapies in patients with acute
930 traumatic brain injury. CNS Drugs 26:613-636.
931 Mikita J, Dubourdieu-Cassagno N, Deloire MS, Vekris A, Biran M, Raffard G,
932 Brochet B, Canron MH, Franconi JM, Boiziau C, Petry KG (2011) Altered
933 M1/M2 activation patterns of monocytes in severe relapsing
934 experimental rat model of multiple sclerosis. Amelioration of clinical
935 status by M2 activated monocyte administration. Mult Scler 17:2-15.
936 Myer DJ, Gurkoff GG, Lee SM, Hovda DA, Sofroniew MV (2006) Essential
937 protective roles of reactive astrocytes in traumatic brain injury. Brain
938 129:2761-2772.
939 Oliva AA, Kang Y, Sanchez-Molano J, Furones C, Atkins CM (2011) STAT3
940 signaling after traumatic brain injury. Journal of neurochemistry.
941 Paintlia MK, Paintlia AS, Singh AK, Singh I (2013) S-nitrosoglutathione induces
942 ciliary neurotrophic factor expression in astrocytes, which has
943 implications to protect the central nervous system under pathological
944 conditions. J Biol Chem 288:3831-3843.
945 Pestka S (2007) The interferons: 50 years after their discovery, there is much
946 more to learn. The Journal of biological chemistry 282:20047-20051.
947 Pineau I, Sun L, Bastien D, Lacroix S (2010) Astrocytes initiate inflammation in
948 the injured mouse spinal cord by promoting the entry of neutrophils and
949 inflammatory monocytes in an IL-1 receptor/MyD88-dependent fashion.
950 Brain, behavior, and immunity 24:540-553.
951 Roth TL, Nayak D, Atanasijevic T, Koretsky AP, Latour LL, McGavern DB (2014)
952 Transcranial amelioration of inflammation and cell death after brain
953 injury. Nature 505:223-228.
954 Sashindranath M, Sales E, Daglas M, Freeman R, Samson AL, Cops EJ, Beckham S,
955 Galle A, McLean C, Morganti-Kossmann C, Rosenfeld JV, Madani R, Vassalli
956 JD, Su EJ, Lawrence DA, Medcalf RL (2012) The tissue-type plasminogen
957 activator-plasminogen activator inhibitor 1 complex promotes
958 neurovascular injury in brain trauma: evidence from mice and humans.
959 Brain : a journal of neurology 135:3251-3264.
960 Sato M, Hata N, Asagiri M, Nakaya T, Taniguchi T, Tanaka N (1998) Positive
961 feedback regulation of type I IFN genes by the IFN-inducible transcription
962 factor IRF-7. FEBS Lett 441:106-110.
963 Sica A, Schioppa T, Mantovani A, Allavena P (2006) Tumour-associated
964 macrophages are a distinct M2 polarised population promoting tumour
965 progression: potential targets of anti-cancer therapy. Eur J Cancer 42:717-
966 727.
967 Summers CR, Ivins B, Schwab KA (2009) Traumatic brain injury in the United
968 States: an epidemiologic overview. Mt Sinai J Med 76:105-110.
969 Taylor JM, Minter MR, Newman AG, Zhang M, Adlard PA, Crack PJ (2014) Type-1
970 interferon signaling mediates neuro-inflammatory events in models of
971 Alzheimer's disease. Neurobiol Aging 35:1012-1023.
972 Terai K, Iwai A, Kawabata S, Sasamata M, Miyata K, Yamaguchi T (2001)
973 Apolipoprotein E deposition and astrogliosis are associated with
974 maturation of beta-amyloid plaques in betaAPPswe transgenic mouse:
975 Implications for the pathogenesis of Alzheimer's disease. Brain research
976 900:48-56.

977 Truettner JS, Suzuki T, Dietrich WD (2005) The effect of therapeutic hypothermia
978 on the expression of inflammatory response genes following moderate
979 traumatic brain injury in the rat. Brain research 138:124-134.
980 Wang G, Zhang J, Hu X, Zhang L, Mao L, Jiang X, Liou AK, Leak RK, Gao Y, Chen J
981 (2013) Microglia/macrophage polarization dynamics in white matter
982 after traumatic brain injury. J Cereb Blood Flow Metab 33:1864-1874.
983 Wang R, Yang B, Zhang D (2011) Activation of interferon signaling pathways in
984 spinal cord astrocytes from an ALS mouse model. Glia 59:946-958.
985 Winer J, Jung CK, Shackel I, Williams PM (1999) Development and validation of
986 real-time quantitative reverse transcriptase-polymerase chain reaction
987 for monitoring gene expression in cardiac myocytes in vitro. Anal
988 Biochem 270:41-49.
989 Yu YJ, Zhang Y, Kenrick M, Hoyte K, Luk W, Lu Y, Atwal J, Elliott JM, Prabhu S,
990 Watts RJ, Dennis MS (2011) Boosting brain uptake of a therapeutic
991 antibody by reducing its affinity for a transcytosis target. Sci Transl Med
992 3:84ra44.
993 Yushkevich PA, Piven J, Hazlett HC, Smith RG, Ho S, Gee JC, Gerig G (2006) User-
994 guided 3D active contour segmentation of anatomical structures:
995 significantly improved efficiency and reliability. Neuroimage 31:1116-
996 1128.
997 Zamanian JL, Xu L, Foo LC, Nouri N, Zhou L, Giffard RG, Barres BA (2012)
998 Genomic analysis of reactive astrogliosis. The Journal of neuroscience :
999 the official journal of the Society for Neuroscience 32:6391-6410.
1000

1001 **Disclosure Statement**

1002 The authors declare that they have no financial or personal conflicts of interest

1003 that relate to this study.

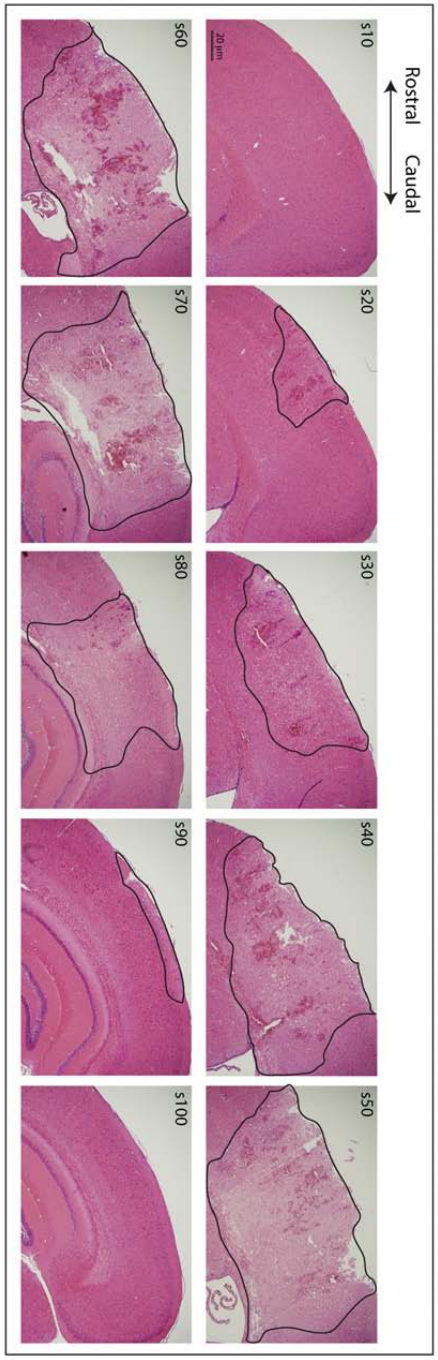
Rostral
Caudal
s10
s20
s30
s40
s50
20 µm
s60
s70
s80
s90
s100

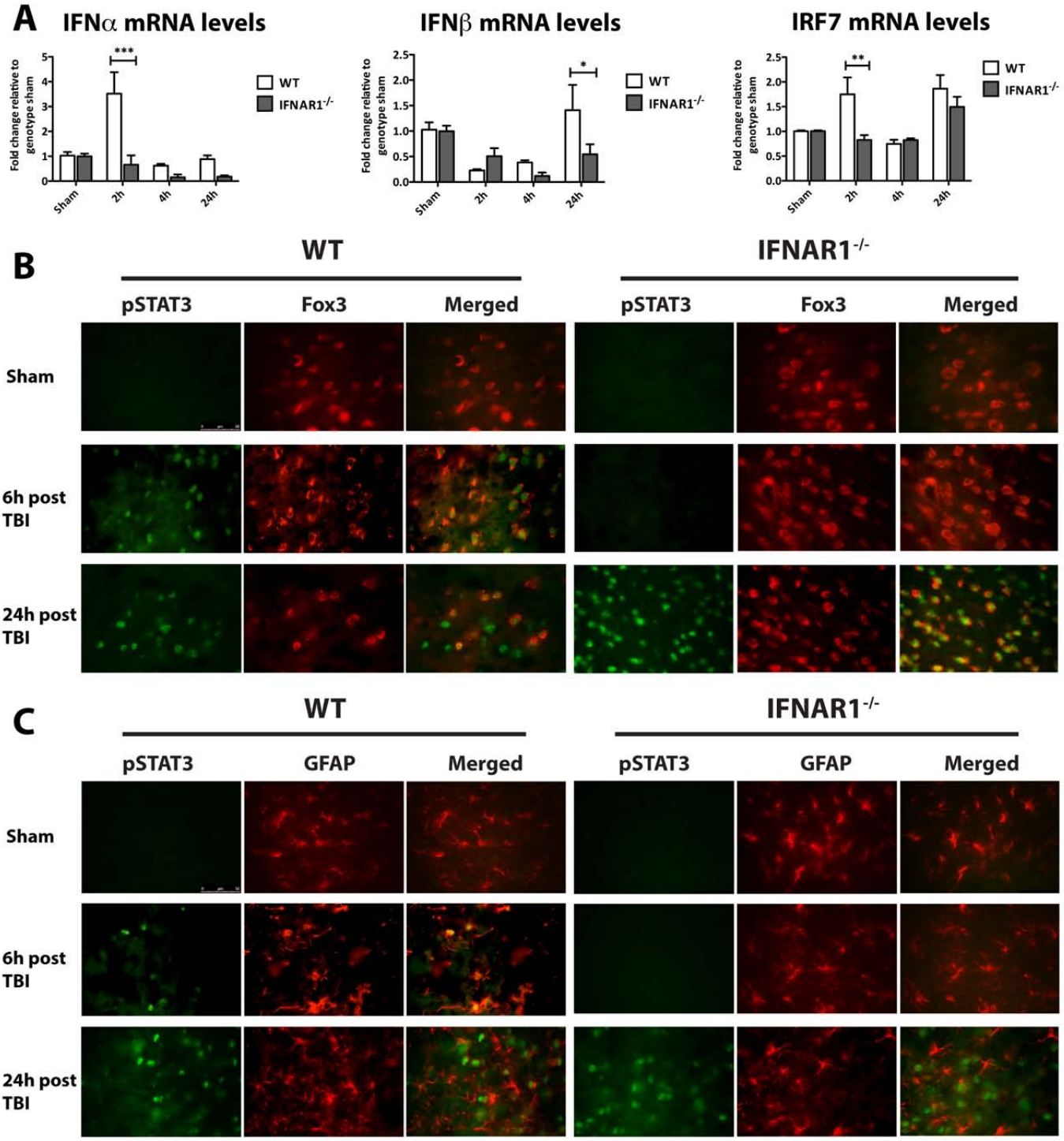

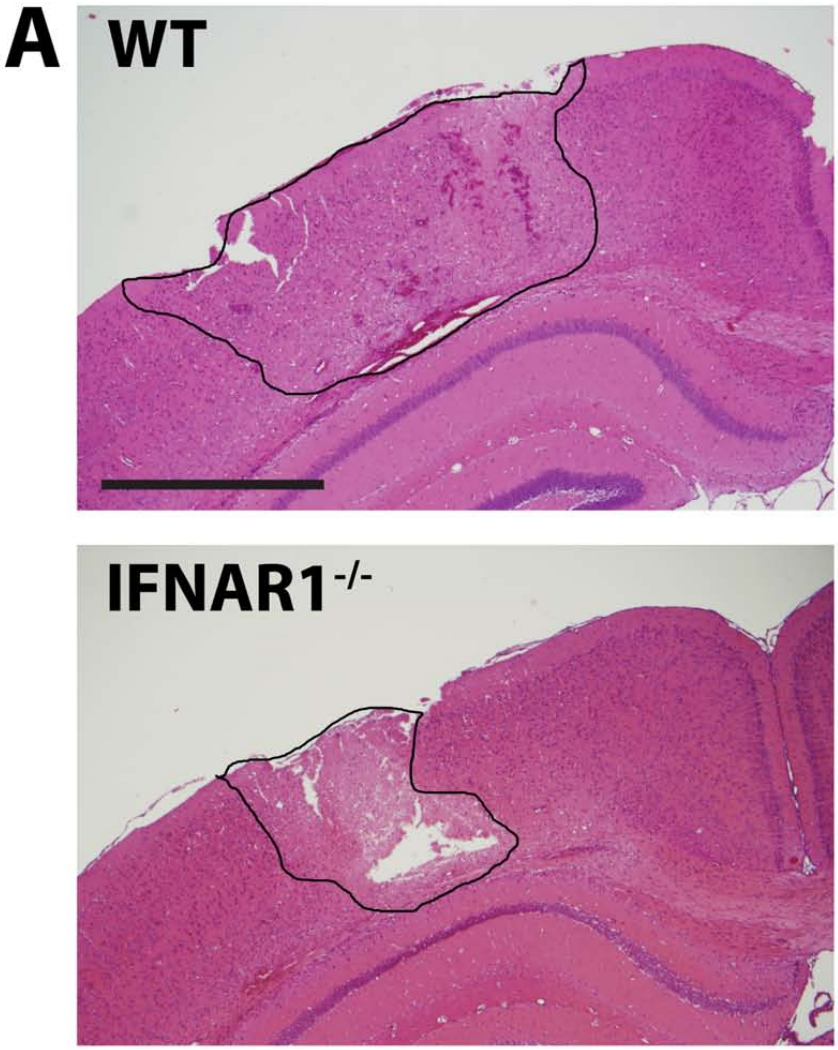

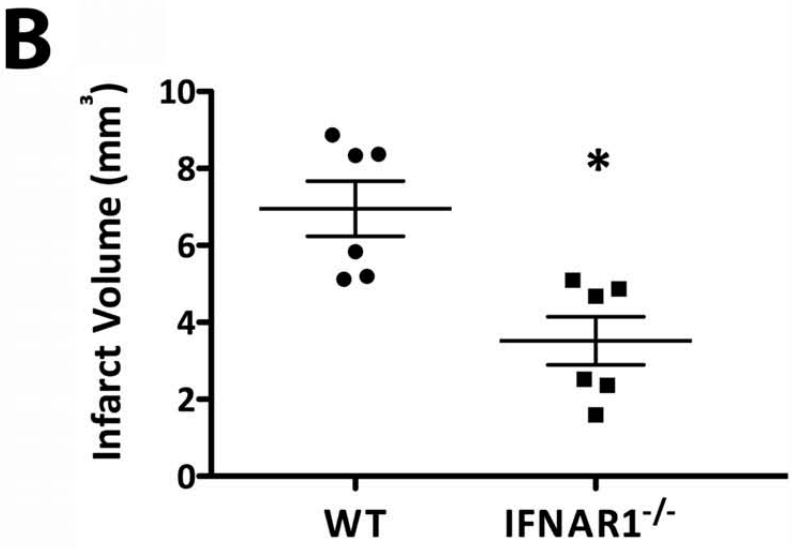

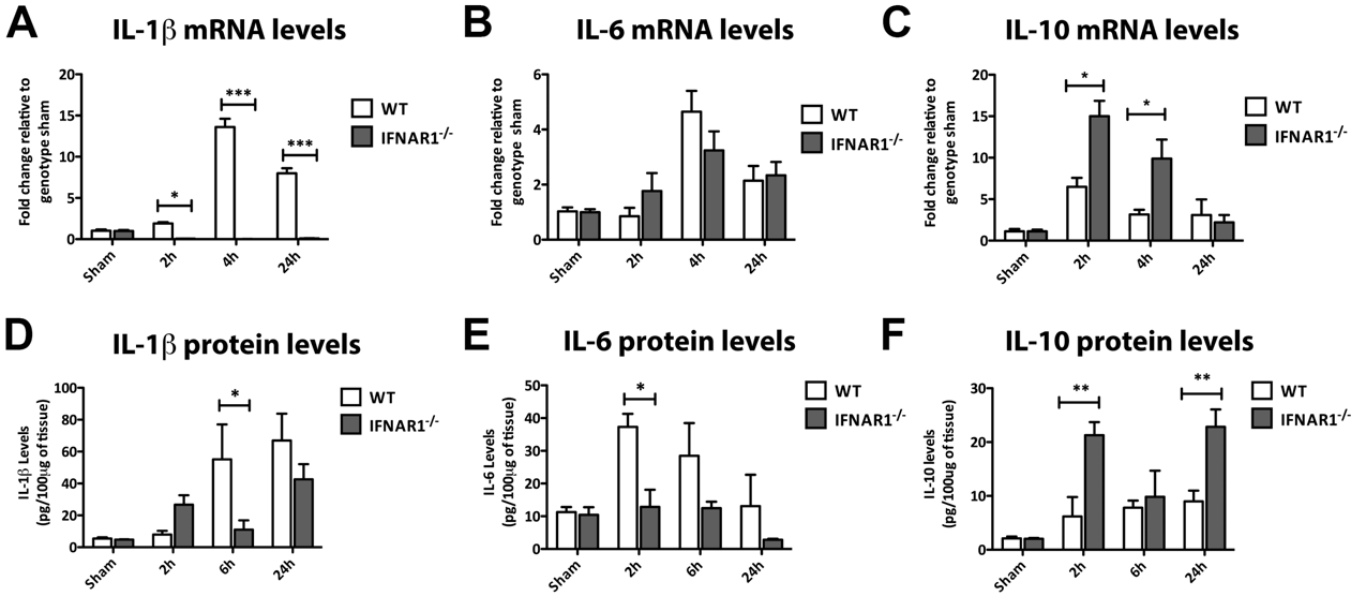

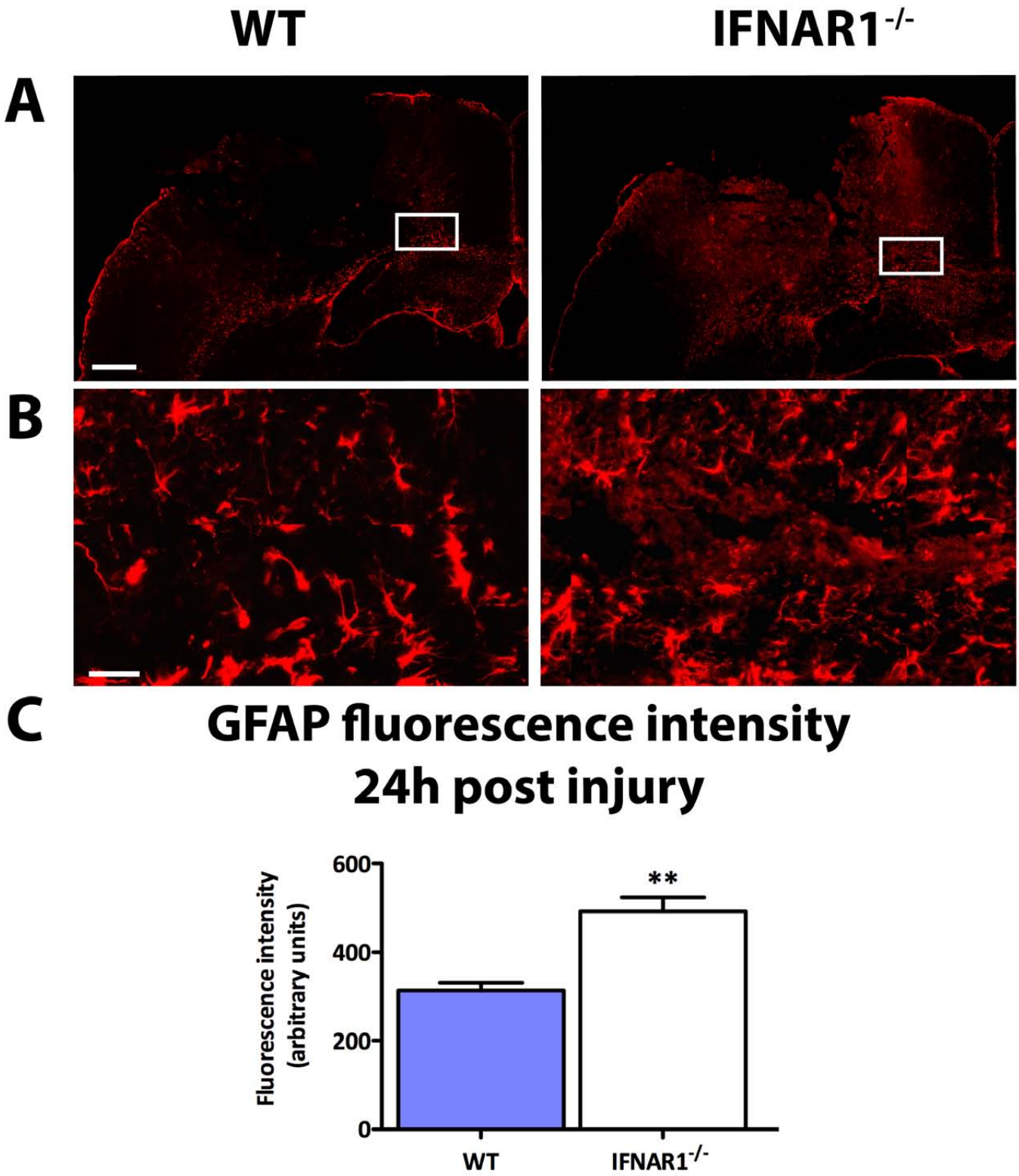

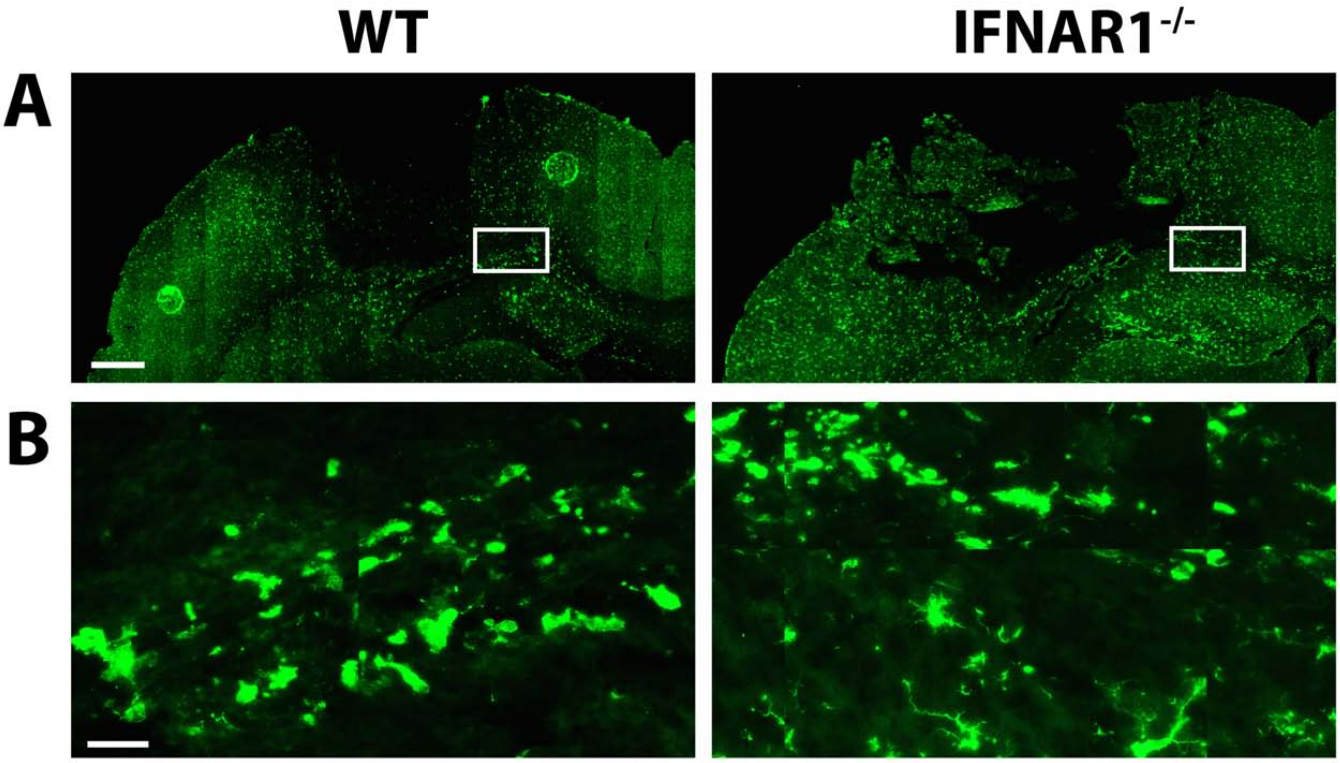

C

Iba-1 fluorescence intensity 24h post injury

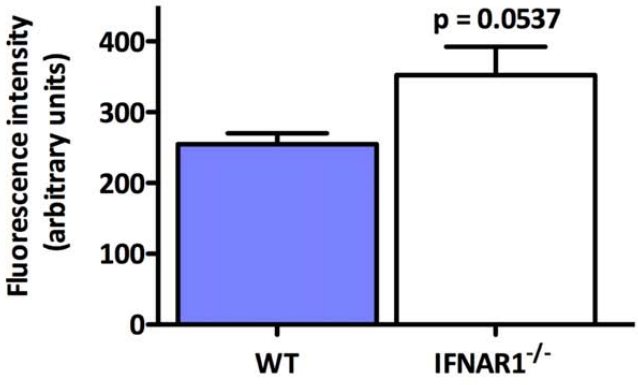

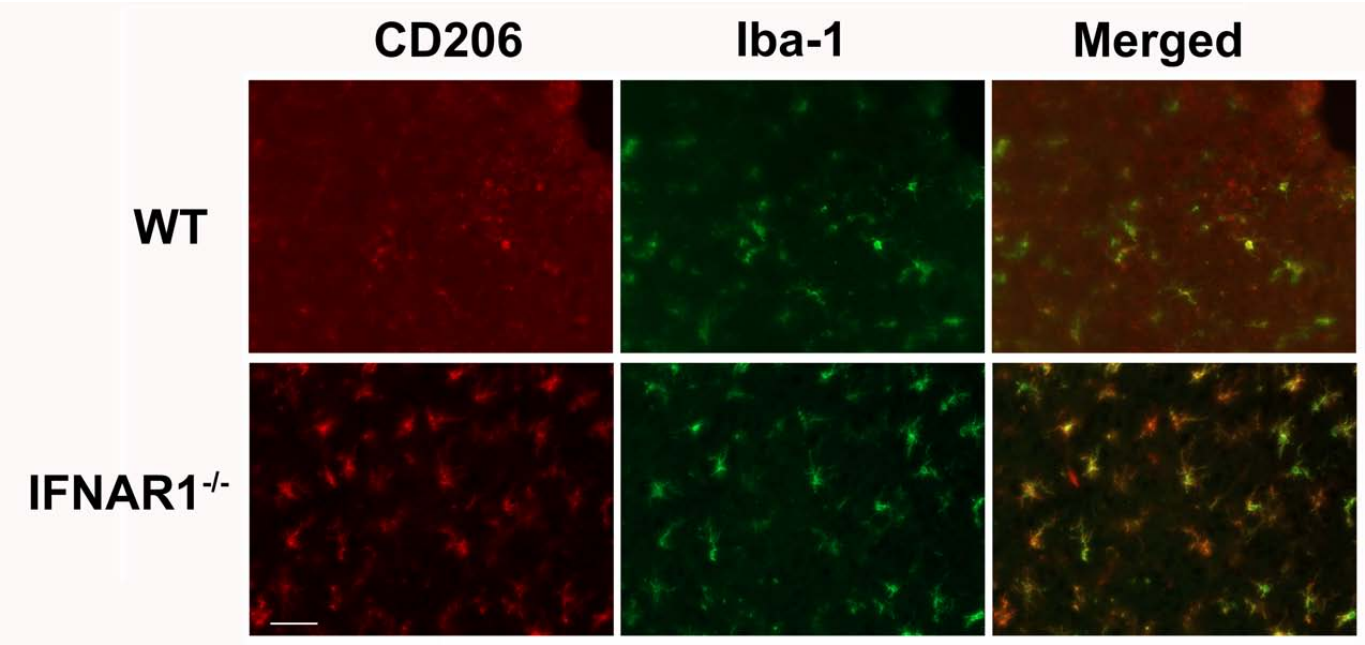

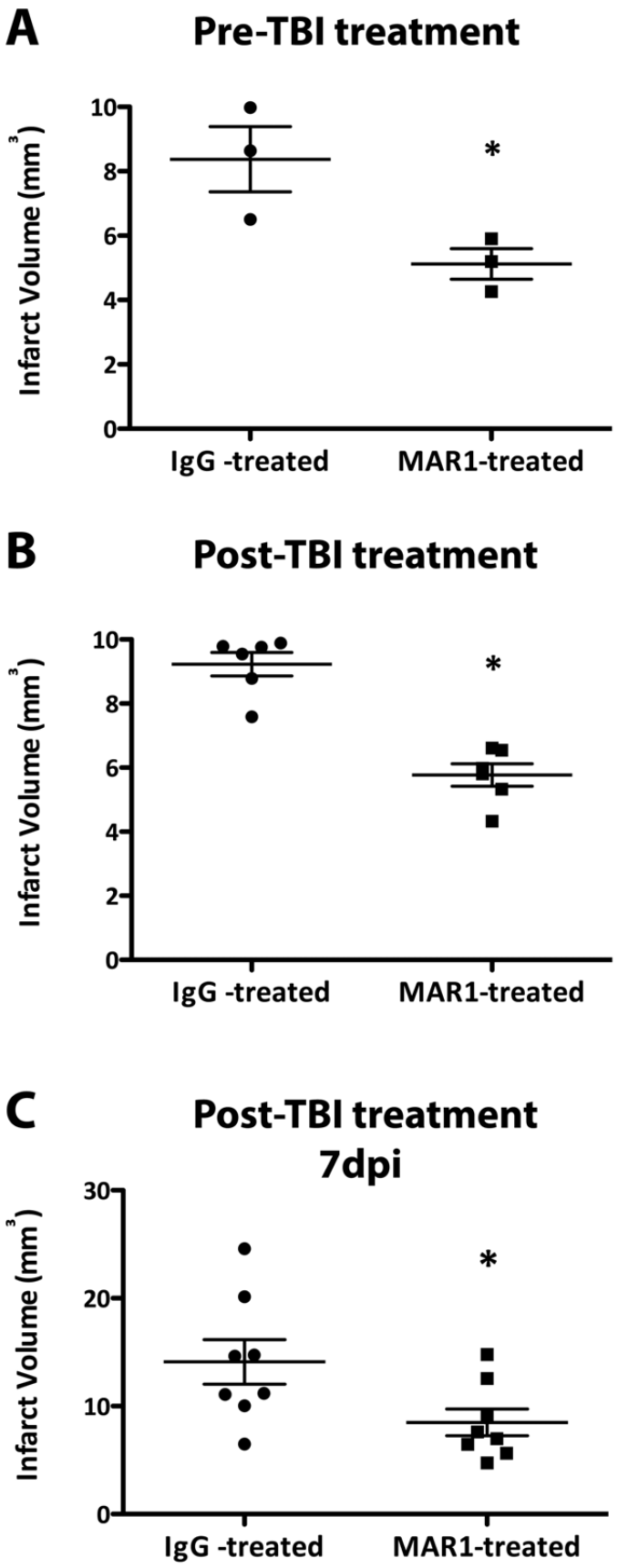

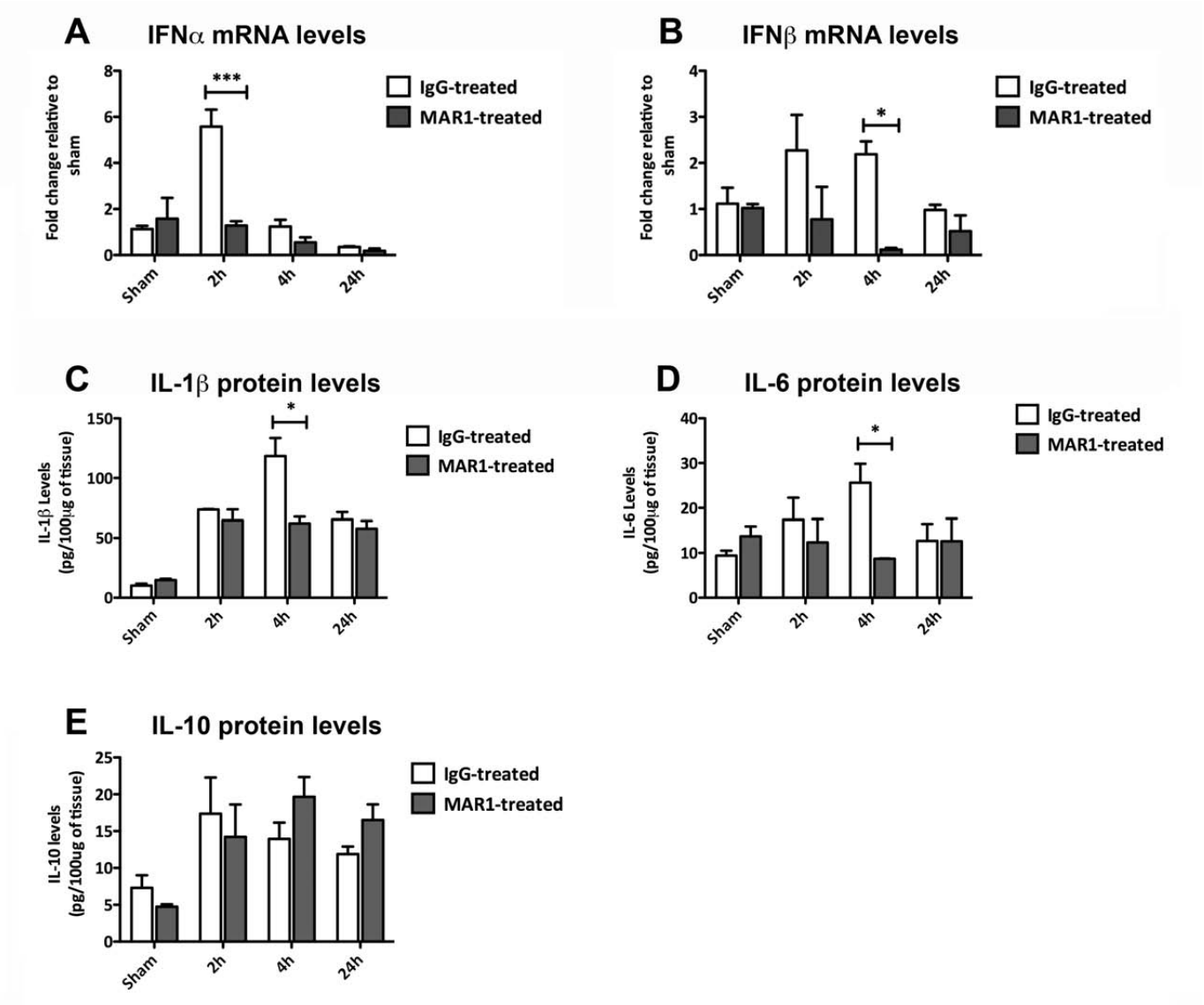

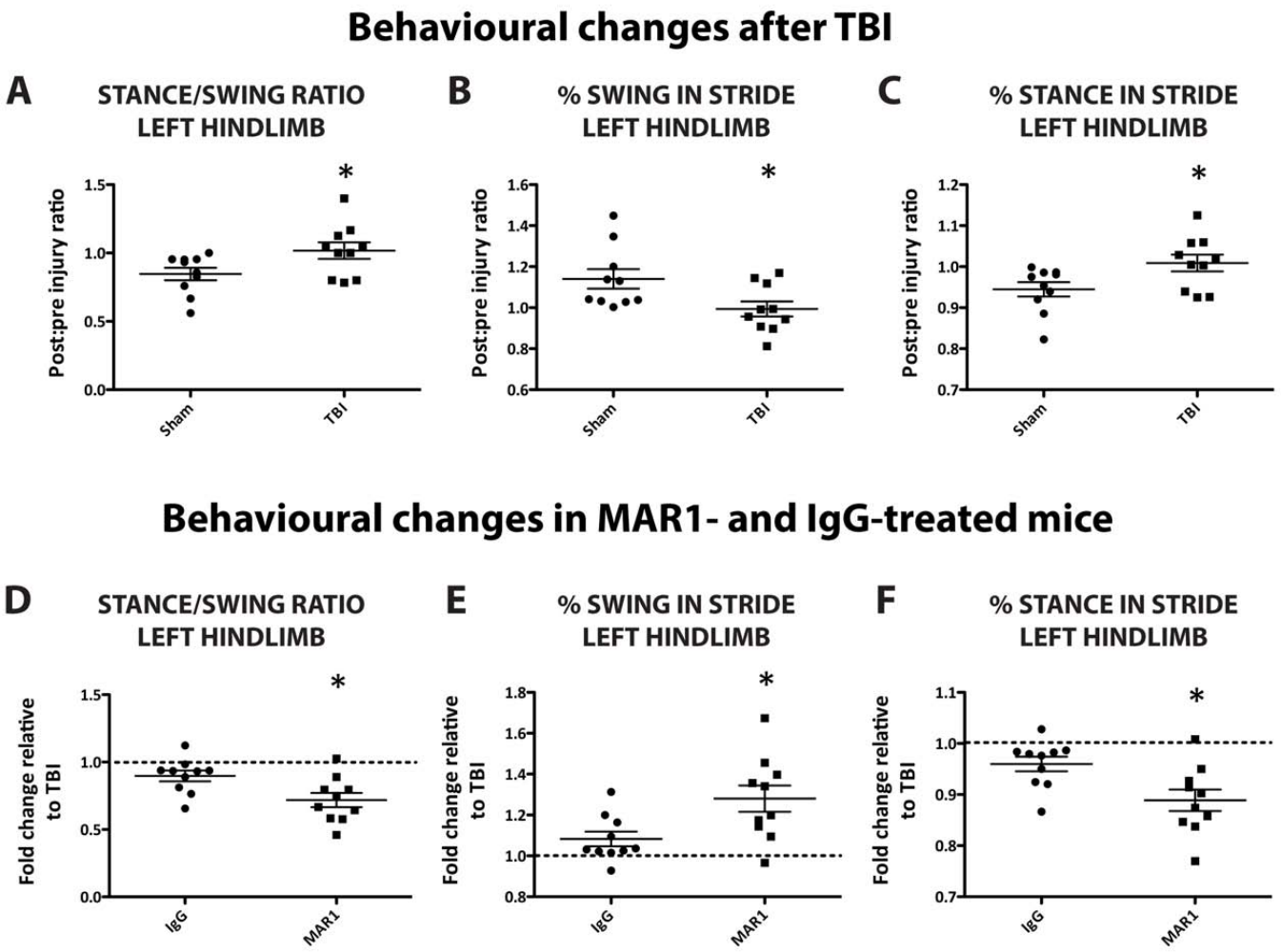

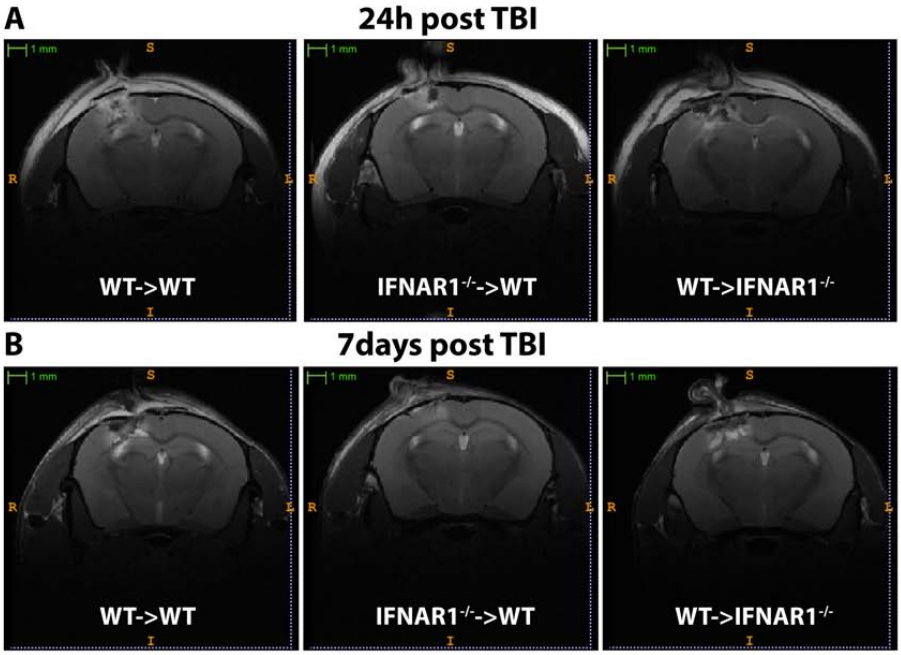

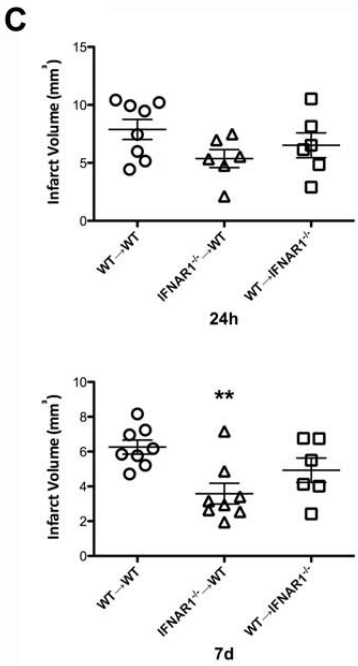

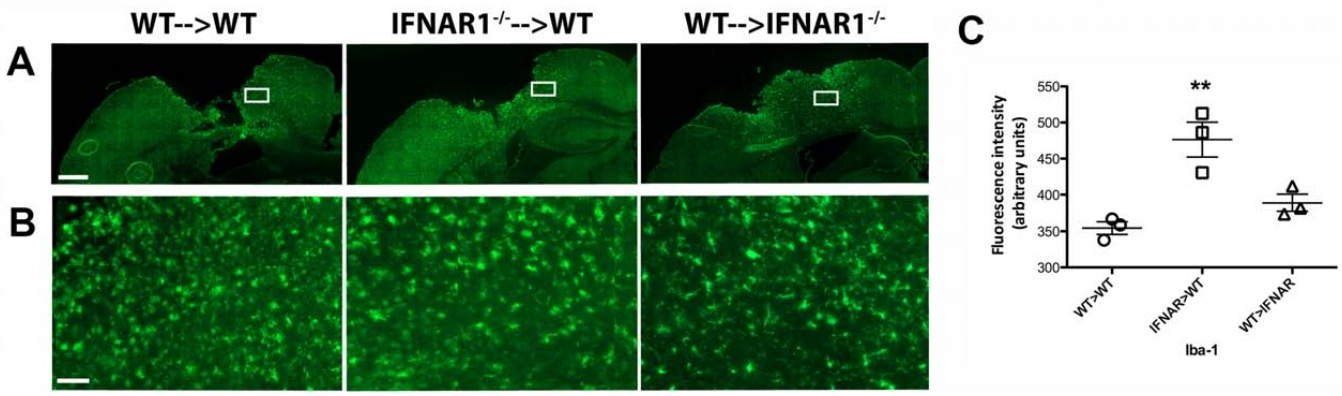

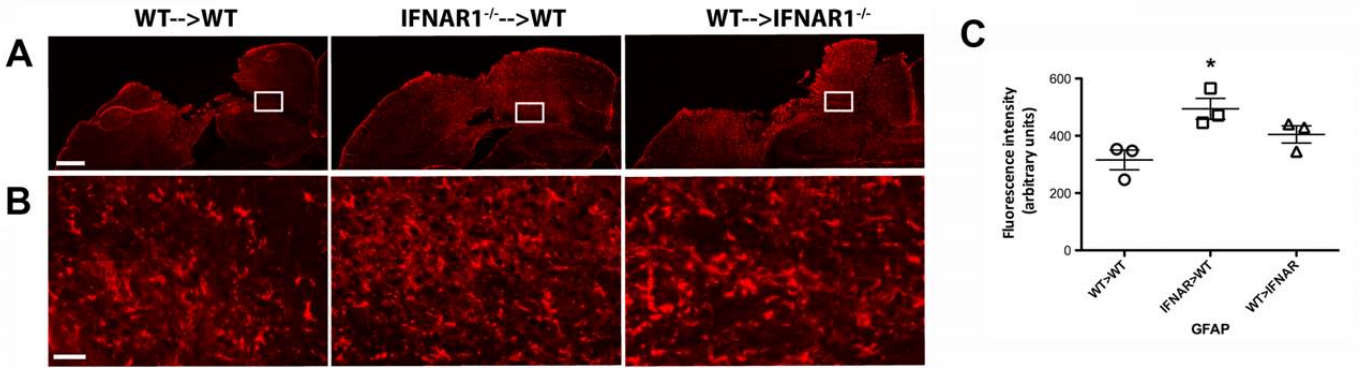

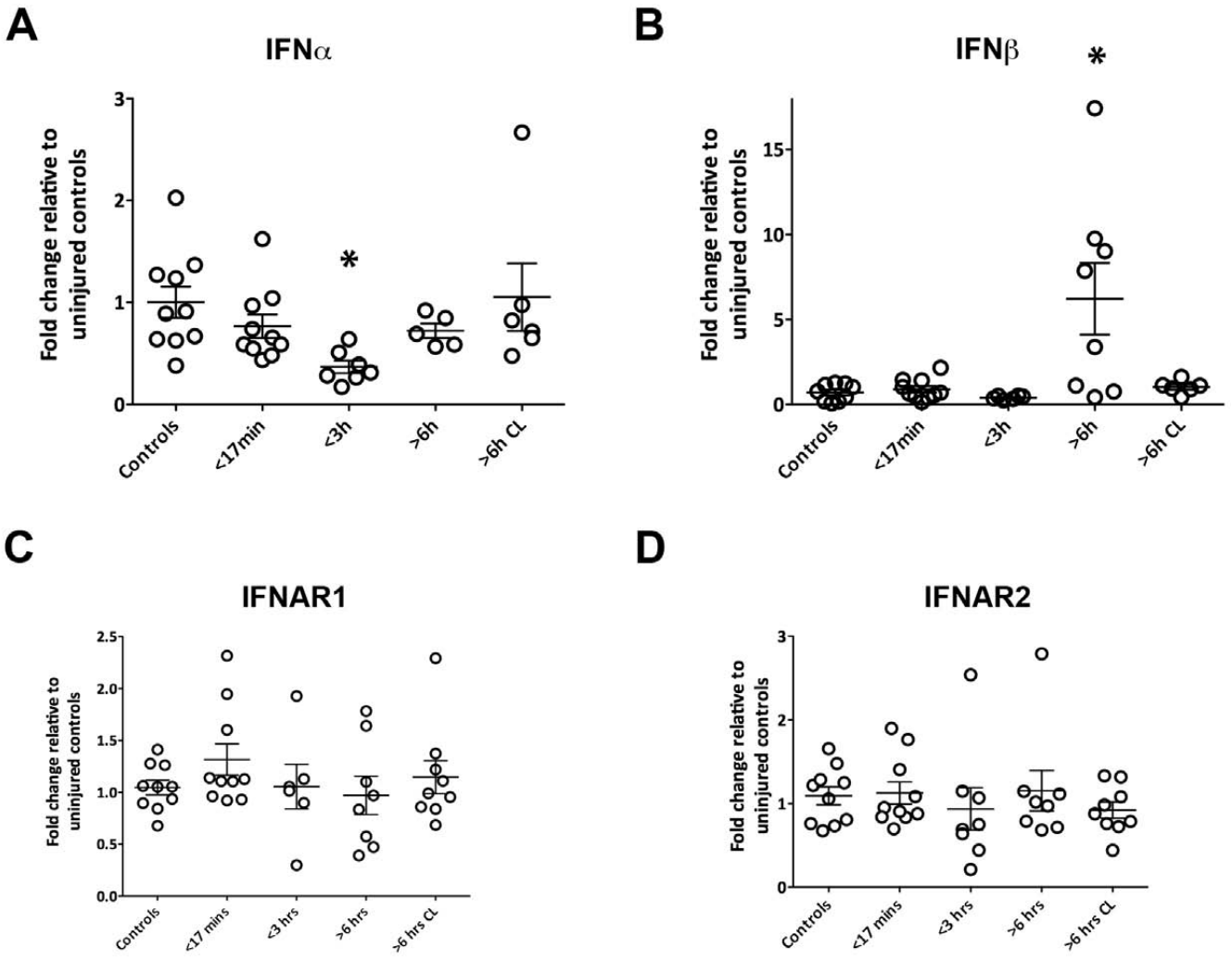

Table 1: Details of trauma and non trauma control cases.

TABLE: Details of 27 trauma and 10 control cases

Case	Age	Sex	Cause of Injury	PMI, h	Cause of death	Survival time
1	51	M	Motor vehicle accident	60	Brain + multiple injuries	< 17 mins
2	63	M	Household accident	70	Brain injury	< 17 mins
3	27	M	Suicide	84	Brain + multiple injuries	< 17 mins
4	41	M	Suicide	96	Brain + multiple injuries	< 17 mins
5	57	F	Motor vehicle accident	87	Brain + multiple injuries	< 17 mins
6	49	M	Motor vehicle accident	107	Brain + multiple injuries	< 17 mins
7	45	M	Motor vehicle accident	43	Brain + multiple injuries	< 17 mins
8	21	M	Motor vehicle accident	100	Brain injury	< 17 mins
9	41.3	M	Aviation accident	114	Brain + multiple injuries	< 17 mins
10	57.6	F	Motor vehicle accident	97	Brain injury	< 17 mins
11	16.8	M	Motor vehicle accident	85	Brain + multiple injuries	< 3 hrs
12	78.7	M	Household accident	45	Brain injury	< 3 hrs
13	18.3	M	Motor vehicle accident	79	Brain + multiple injuries	< 3 hrs
14	34.7	M	Motorbike accident	66	Brain + multiple injuries	< 3 hrs
15	22.9	F	Motor vehicle accident	108	Brain + multiple injuries	< 3 hrs
16	52.8	M	Motorbike accident	65	Brain + multiple injuries	< 3 hrs
17	19.6	M	Suicide	33	Brain + multiple injuries	< 3 hrs
18	59.8	M	Motor vehicle accident	71	Brain + multiple injuries	< 3 hrs
19	46.0	M	Fall	129	Brain injury	6 hrs
20	56.3	M	Motor vehicle accident	65	Brain injury	8 hrs
21	64.6	M	Fall	61	Brain injury	8 hrs
22	75.9	M	Staircase fall	89	Brain injury	10 hrs
23	59.6	F	Motor vehicle accident	80	Brain injury	35 hrs
24	61.7	M	Fall	40	Brain injury	93 hrs
25	38.9	F	Staircase fall	101	Brain injury	122 hrs
26	70.9	M	Motor vehicle accident	114	Brain injury	76 hrs
27	73.7	M	Fall	91	Brain injury	29 hrs
Controls						
28	16	M	-	-	Suicide by hanging	-
29	48.7	M	-	50	Cardiac failure	-
30	51.6	M	-	64	Asthma	-
31	52.3	M	-	52	Cardiomyopathy	-
32	59.6	M	-	43	Pulmonary embolism	-
33	64.1	M	-	24	Ischaemic heart disease	-
34	66.9	M	-	10	Pneumonia	-
35	64.4	M	-	24	Pulmonary embolism	-
36	77.5	M	-	53	Myocardial infarction	-
37	60	F	-	48	Myocardial infarction	-

Cases 1-10: cases with a survival time between 0 and 17 minutes; Cases 11-18: cases with a survival time between 30 minutes and 3 hours; Cases 19-27: cases with a survival time between 6 and 261 hours; Cases 28-37: control cases. All brains were obtained at autopsy. PMI, *post mortem* interval (time between death and brain retrieval); M, male; F, female.

Table 2. Summary of statistics from figures
Statistical analysis was performed using GraphPad Prism6.

Figure	Panel	Data structure#	Test type	p value
1	A^{i}	normal	2-way Anova, Bonferoni post-hoc	$p<0.05$
	A^{ii}	normal	2-way Anova, Bonferoni post-hoc	$p<0.001$
	A^{iii}	normal	2-way Anova, Bonferoni post-hoc	$p<0.01$
2	B	normal	Students t-test	$p=0.0047$
3	A	normal	2-way Anova, Bonferoni post-hoc	$p<0.001$
	C	normal	2-way Anova, Bonferoni post-hoc	$p<0.05$
	D	normal	2-way Anova, Bonferoni post-hoc	$p<0.05$
	E	normal	2-way Anova, Bonferoni post-hoc	$p<0.05$
	F	normal	2-way Anova, Bonferoni post-hoc	$p<0.01$
4	C	normal	Students t-test	$p=0.001$
5	C	normal	Students t-test	$p=0.0537$
6	A	normal	Students t-test	$p=0.0438$
	B	normal	Students t-test	$p=0.0001$
	C	normal	Students t-test	$p=0.0353$
7	A	normal	2-way Anova, Bonferoni post-hoc	$p<0.001$
	B	normal	2-way Anova, Bonferoni post-hoc	$p<0.05$
	C	normal	2-way Anova, Bonferoni post-hoc	$p<0.05$
	D	normal	2-way Anova, Bonferoni post-hoc	$p<0.05$
8	A	normal	Students t-test	$p=0.0277$
	B	normal	Students t-test	$p=0.0255$
	C	normal	Students t-test	$p=0.0288$
	D	normal	Students t-test	$p=0.0124$
	E	normal	Students t-test	$p=0.0156$
	F	normal	Students t-test	$p=0.0153$
9	C	normal	One-way Anova, Dunnett post-hoc	$p=0.0003$
10	C	normal	One-way Anova, Dunnett post-hoc	$p=0.0273$
11	C	normal	One-way Anova, Dunnett post-hoc	$p=0.0047$
12	A	normal	One-way Anova, Dunnett post-hoc	$p=0.0019$
	B	normal	One-way Anova, Dunnett post-hoc	$p=0.0001$

Kolmogorov-Smirnov test (with Lilliefors correction) was used to test for normality within each group.